TABLE OF CONTENTS - Appendix J

List of Figures ..... J–ii

List of Tables ..... J–i

Appendix J
Interim Report on Experiments to Support Fire Dynamics and Thermal Response Modeling J–1

J.1 Introduction J–1

J.2.1 Description of Experiments J–2

J.2.2 Preliminary Results J–7

J.3 Experiments for Guiding the FDS Fire Growth Predictions J–12

J.3.1 Description of the Experiments J–12

J.3.2 Preliminary Results J–18

J.4 Experiments for Fire Model Validation J–27

J.4.1 Preliminary Results J–32

J.5 References J–34

Attachment 1
Simulating the Fires in the World Trade Center J–35

LIST OF FIGURES

Figure J–1. Experimental enclosure during construction, viewed with access panels removed. J–3
Figure J–2. Compartment content layout J–4
Figure J–3. Tubular column. J–5
Figure J–4. Bar joist. J–5
Figure J–5. Simple bar. J–6
Figure J–6. Measured heat release rate as a function of time during tests 1–6. .....J–7
Figure J–7. Temperature-time history for truss A in test 5. .....J–8
Figure J–8. Temperature-time history for truss A in test 3. .....J–9
Figure J–9. Comparison of gas temperatures, test 3, exhaust side of compartment. J–10
Figure J–10. Comparison of gas temperatures, test 5, exhaust side of compartment. J–10
Figure J–11. Comparison of heat fluxes to column, test 3. .....J–11
Figure J–12. Comparison of heat fluxes to column, test 5. .....J–11
Figure J–13. Photograph of right side of generic workstation. J–13
Figure J–14. Photograph of left side of generic workstation. J–13
Figure J–15. Photographs of high-end workstation. J–15
Figure J–16. Photograph of workstation soon after ignition in test 2. .....J–18
Figure J–17. Photograph of workstation near the peak heat release rate in test 2. .....J–19
Figure J–18. Heat release rate versus time for single workstation test 1. .....J–19
Figure J–19. Heat release rate versus time for single workstation test 2. .....J–20
Figure J–20. Heat release rate versus time for single workstation test 3. .....J–20
Figure J–21. Heat release rate versus time for single workstation test 4. .....J–21
Figure J–22. Heat release rate versus time for single workstation test 5. .....J–21
Figure J–23. Heat release rate versus time for single workstation test 6. .....J–22
Figure J–24. Preliminary comparison of predicted and measured HRR values. J–26
Figure J–25. Plan view of test configuration. J–28
Figure J–26. Elevation view of test configuration. J–29
Figure J–27. Views of interior of test fixture. J–30
Figure J–28. View of fire compartment before the start of test 6. .....J–33
Figure J–29. View of fire compartment 2 minutes after the start of test 6. .....J–33
Figure J–30. Fire Dynamics Simulator 3D rendition of experimental enclosure. J–34
Figure J–31. Comparison of measured and predicted heat release rate for test 1. .....J–34

LIST OF TABLES

Table J–1. Test matrix. J–6
Table J–2. Summary of insulation on steel components.....J–6
Table J–3. Peak heat release rates and times to peak.....J–22
Table J–4. Test matrix. J–31

This page intentionally left blank.

Appendix J
INTERIM REPORT ON EXPERIMENTS TO SUPPORT FIRE DYNAMICS AND THERMAL RESPONSE MODELING

J.1 INTRODUCTION

The reconstruction of the World Trade Center (WTC) fires involves two computation models:

- Fire Dynamics Simulator (FDS): This is the first large-domain CFD fire model that predicts and visualizes the spread, growth and suppression of a fire based on the underlying scientific principles governing fluid motion. The model numerically solves the conservation equations of mass, momentum and energy that govern low-speed, thermally driven flows with an emphasis on smoke and heat transport from fires. The companion software package, called Smokeview, graphically presents the results of the FDS three-dimensional (3D) time-dependent simulation. Smokeview animates in three dimensions the smoke particulates, heat fluxes, temperatures and fluid velocities within a building. Users of the package can view the enclosure from any angle and from inside or outside.

- Fire-Structure Interface (FSI): This code effects the transfer of radiant and convective heat from a CFD fire model, such as FDS, to a coupled, transient, three-dimensional finite element model for the thermal response of structural members, such as ANSYS. The members may be simple (e.g., bare steel) or complex (e.g., insulation-coated steel).

For application to the Investigation, each of these needs experimental data (a) to guide adaptation/development of the models for this specific purpose and (b) with which to ascertain the accuracy of the model predictions. Ideally the uncertainty in the agreement with experiments will be much smaller than the effect of varying the unknowns in the actual conditions on September 11, 2001.

The following text describes three sets of experiments designed to accomplish this. All three sets have been completed, and the analysis of the data is under way. Full reports are in preparation and will be completed in summer 2004. Attachment 1 is a short paper on the modeling and experiments that will be presented at Interflam in July 2004.

J.2 EXPERIMENTS FOR ACCURACY ASSESSMENT OF THERMAL ENVIRONMENT MODELING

The purposes of these experiments, conducted in the National Institute of Standards and Technology (NIST) Large-scale Fire Laboratory from March 10 through 26, 2003, were to:

- Assess the accuracy with which FDS predicts the thermal environment in a burning compartment and;

- Establish a data set to validate the prediction of the temperature rise of structural steel elements using FSI.

Within a large test compartment, assorted steel members were exposed to controlled fires of varying heat release rate (HRR) and radiative intensity. The steel members were bare or coated with spray-applied fireproofing of two thicknesses. The thermal profile of the fire was measured at multiple locations within the compartment. Temperatures were also recorded at multiple locations on the surfaces of the steel, the insulation, and the compartment. Prior to each test, a prediction of the thermal environment in the compartment was determined using FDS. Following the tests, the prediction and experimental results were compared.

J.2.1 Description of Experiments

The test compartment consisted of a steel stud frame lined with calcium silicate board. The internal dimensions of the compartment were 3 m high, 7 m deep, and 4 m wide. There were four openings in the west wall through which air entered the room; they totaled 1.75 m^2 (10.8 ft^2) in area and were located 1 m (3.3 ft) above the floor. There were four openings in the east wall through which heat and combustion products were emitted; they also totaled 1.75 m^2 (10.8 ft^2) in area and were located 2 m above the floor. A photograph is shown in Fig. J–1 and a schematic in Fig. J–2.

In each of the six tests, the four test subjects were a bar, two trusses, and a thin-walled tubular column. These are depicted in Figs. J–3 through J–5. Depending on the test, these specimens were either left unprotected or were coated with spray-applied fire protective insulation material, BlazeShield DC/F. The fibrous insulation was applied by an experienced applicator who took considerable care to apply an even coating of the specified thickness. As such, the insulated test subjects represent a best case in terms of thickness and uniformity.

The fires consisted of liquid hydrocarbon fuels sprayed by a two-nozzle spray burner onto a 1 m × 2 m (3.3 ft × 6.6 ft) pan. The fuels were (a) heptanes and (b) a mixture of nominally 60 percent (by mass) heptanes with 40 percent toluene. The latter fuel produced a significantly sootier flame.

The instrumentation for the tests comprised up to 352 channels of data.

- The combustion products were collected in a 6 m × 6 m (21.5 ft × 21.5 ft) hood. Instrumentation in the exhaust duct enabled calculation of the rate of heat release throughout a test.

- Fourteen heat flux gauges were placed strategically around the compartment to measure the transport of radiant energy; in addition, there were four slug calorimeters measuring the total heat flux parallel to the trusses.

Most of the channels were for thermocouples that measured the temperatures on the surface of the walls and ceiling, within the walls, on the surface of the steel components, and at the surface of the spray-applied insulation. With the large number of measurements, it was possible to go beyond the traditional point-by-point comparison and discover why the model either under- or overpredicted a given measurement. A description of the test series appears in Table J–1. Table J–2 shows the dimensions and

variability of the spray-applied insulation. The measurements were taken at numerous locations along the perimeter and length of each specimen using a pin-thickness gauge specifically designed for this type of insulation.

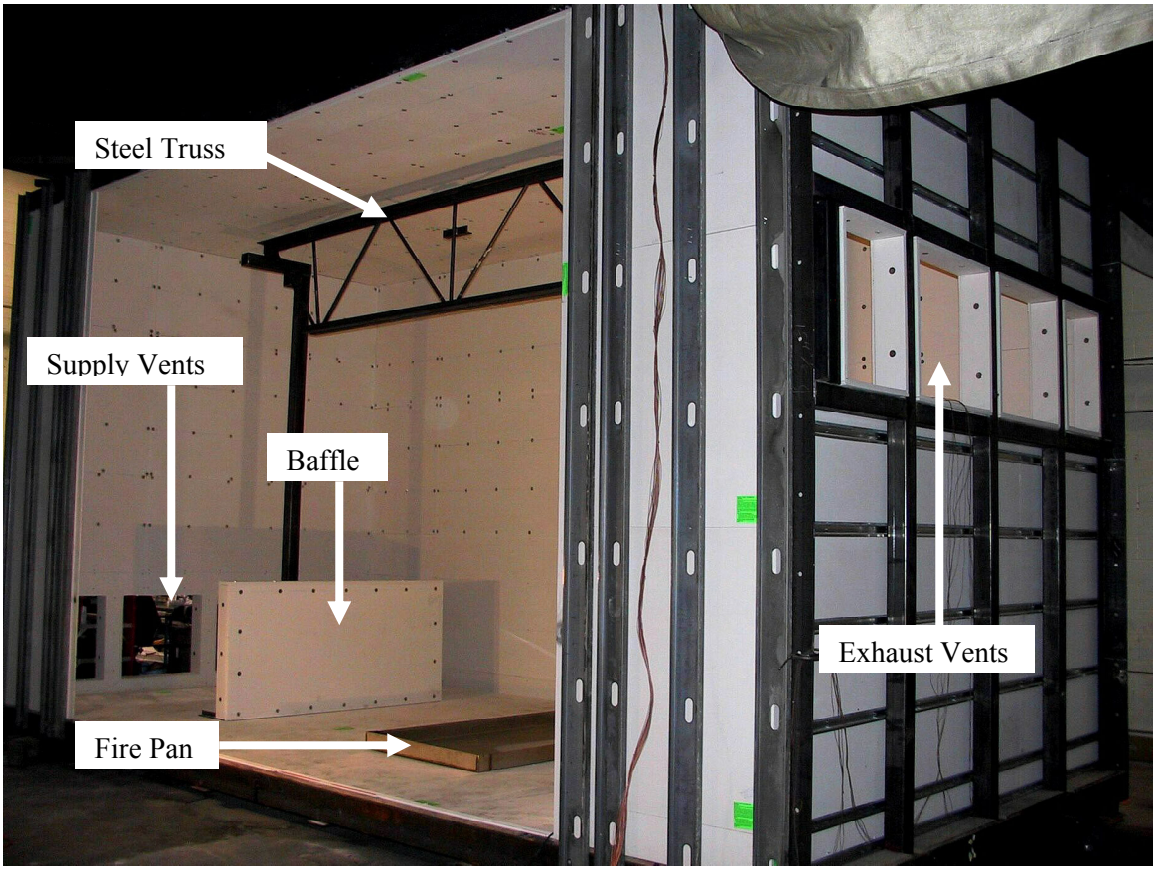

Figure J–1. Experimental enclosure during construction, viewed with access panels removed.

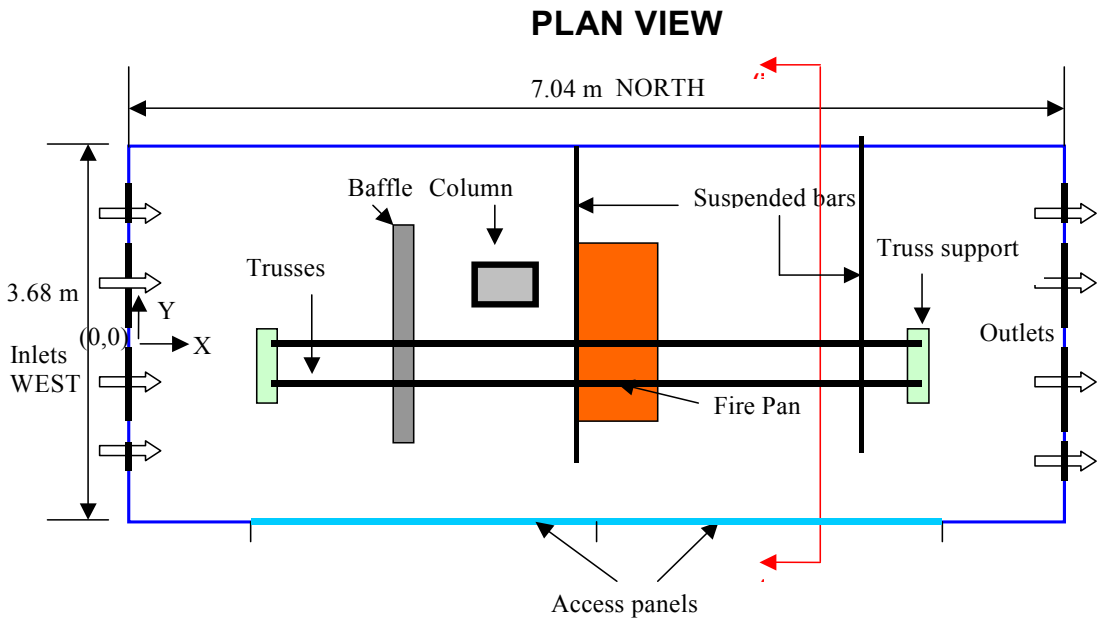

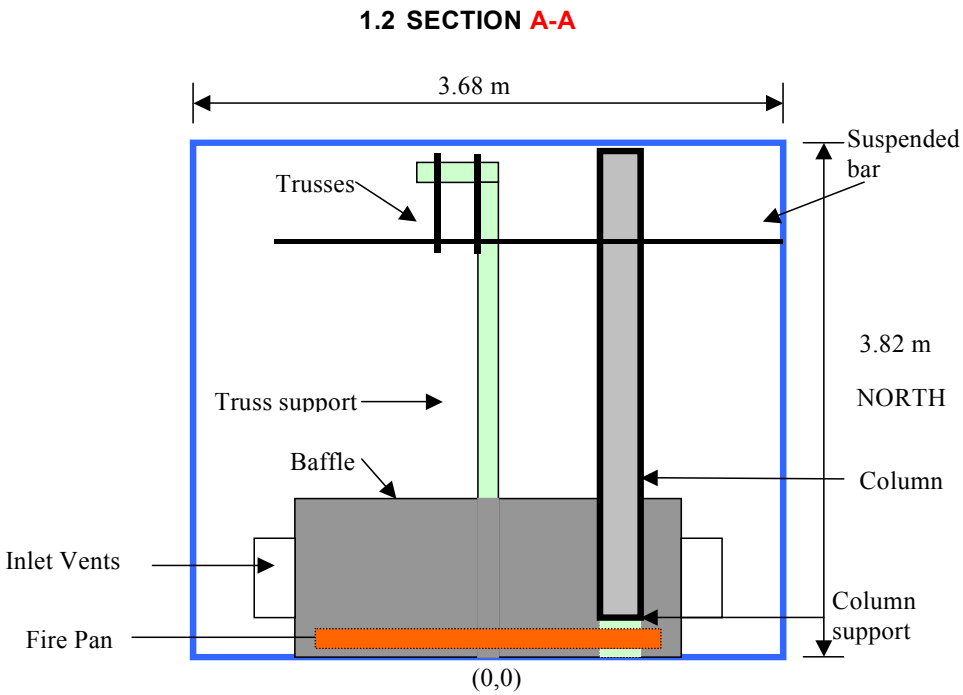

Figure J–2. Compartment content layout (not to scale).

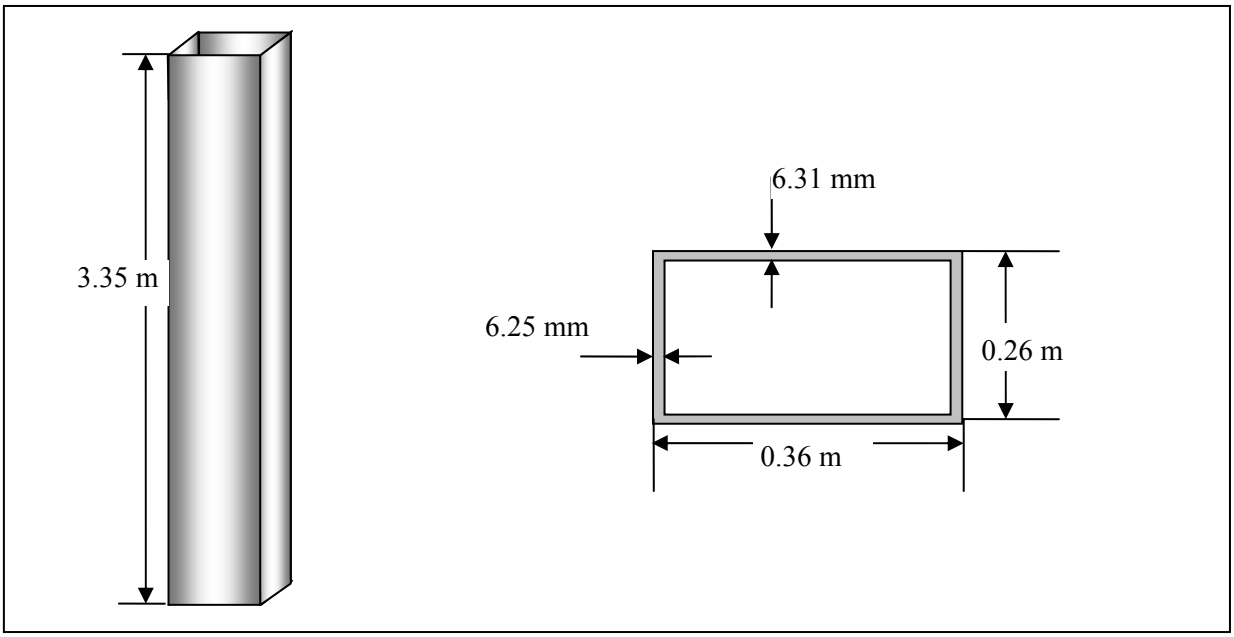

Figure J–3. Tubular column.

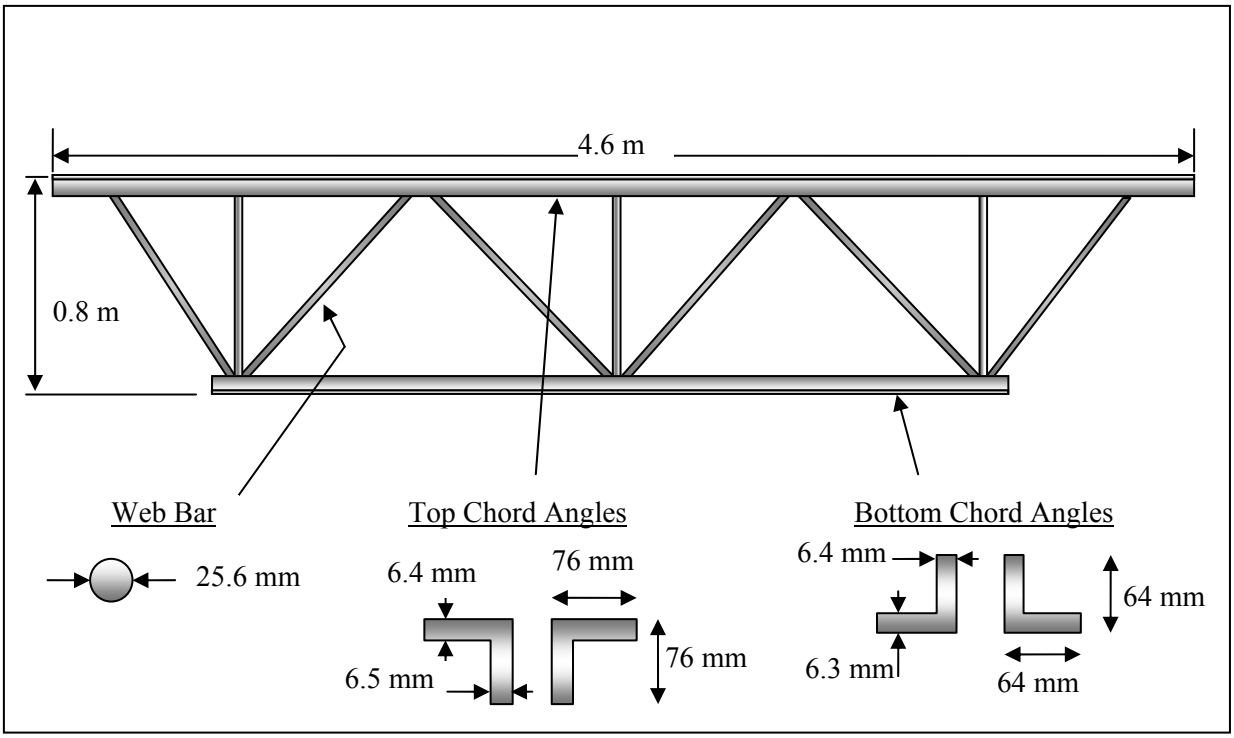

Figure J–4. Bar joist.

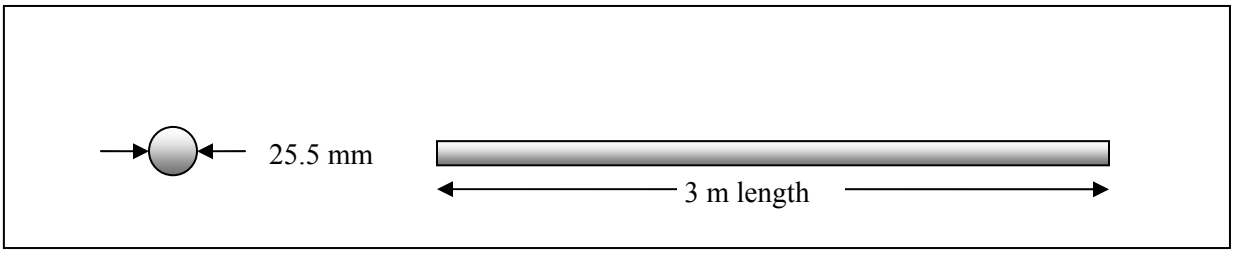

Figure J–5. Simple bar.

Table J–1. Test matrix.

Test	Measured Heat Release Rate (MW)	Fuel	Planned Insulation Thickness (mm)	Planned Test Duration (min)
1	2.0	Heptanes	None	15
2	2.4	Heptanes/toluene	None	15
3	2.0	Heptanes/toluene	None	15
4	3.2	Heptanes	Same as test 5	15
5	3.0	Heptanes	See Table J–2	50
6	3.0	Heptanes	See Table J–2	50

Table J–2. Summary of insulation on steel components.

Test	Item	Specified Thickness (mm)	Applied Thickness (mm)	
			Mean	Std. Deviation
5	Bar	19.1	23.0	5.5
	Column	38.1	41.0	3.0
	Truss A	19.1	26.9	7.3
	Truss B	38.1	40.5	8.2
6	Bar	19.1	25.3	4.6
	Column	19.1	21.4	3.5
	Truss A	19.1	26.0	6.9
	Truss B	19.1	25.6	6.9

The HRR are shown in Fig. J–6. The important features of the HRR curves are:

- The expected (from the calorific value of the fuels) and measured heat release rates agreed within the relative expanded experimental uncertainty of ±11%.
- The heat release rates are steady over the time interval in which the burner was turned on.

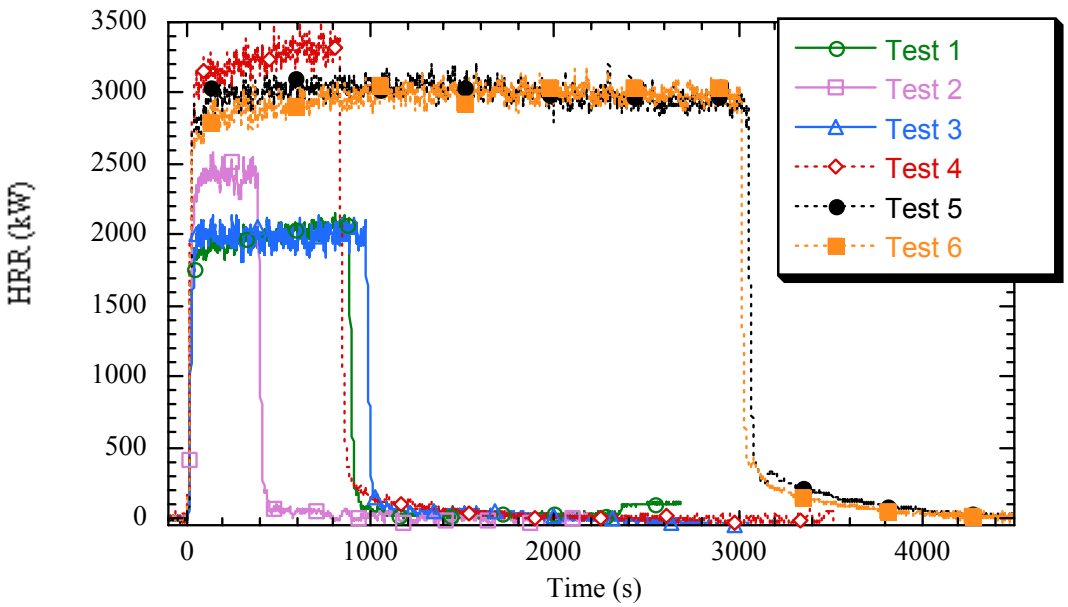

Figure J–6. Measured heat release rate as a function of time during tests 1–6.

In each test, the baseline signals from all the measurement devices were established; then the burner was ignited and continued burning at a steady rate until the temperature at any steel surface approached approximately 600 °C. (Above this temperature, there was concern that loss of strength might lead to collapse and accordant damage to the test facility.) At that point, the burner was turned off. In test 2, the steel reached the target temperature at about 6 min and was terminated at that time. During test 4, the Omega GG glass braid wire thermocouple extension cables failed leading to erroneous thermocouple readings. This was likely due to the opening-up of the Kaowool thermal insulation protective blanket around the thermocouple wires and subsequent shorting. Thus the test was terminated early, and the data have not been processed. To prevent reoccurrence of this problem during tests 5 and 6, the extensions were water cooled and double wrapped with Kaowool insulation. Each layer of Kaowool insulation was secured to the thermocouples using steel wire. Additionally, the thermocouple extensions were rerouted through the cooler west side of the compartment. After tests 5 and 6, the thermocouple extensions were visually inspected and were found to be undamaged.

J.2.2 Preliminary Results

Figure J–7 shows typical temperature data obtained in the tests. These data are for truss A in test 5. The thermocouple location notation is as follows: TU: Truss Upper Chord, TM: Truss Middle (Web), TL: Truss Lower Chord; 1 to 4: locations across the length of the test specimen; S: on the steel surface, I: on the outer surface of the insulation; A: truss A. For the informative nature of this progress report, it is only important to note the following:

- The curves that rise sharply from the beginning of the test are those for temperatures on the outside of the insulation.
- The curves that rise more gently are those for temperatures at the interface between the steel and the insulation.

From the figure, one can see that:

- The 19.1 mm (0.75 in.) insulation delays the rise to a peak steel temperature by almost an hour at all locations.
- The highest temperature reached at the steel surface is approximately 300 °C lower than the temperature at the outside face of the insulation material.

The curve patterns for the other steel specimens in the tests with insulated steel are similar in shape.

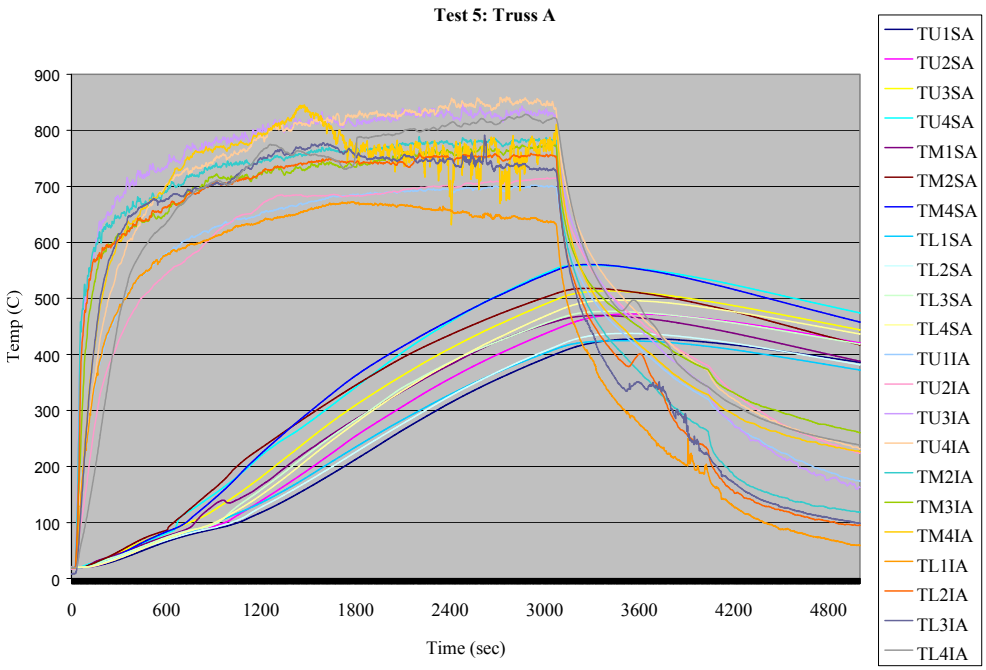

Figure J–7. Temperature-time history for truss A in test 5.

By contrast, Fig. J–8 shows the same plot for truss A from test 3, in which the truss was not insulated and the fire was of shorter duration and lower intensity. Nonetheless, the outer surface of the steel reached the targeted maximum temperature (just short of 600 °C) in about one-third the time. As expected, this result is typical of the fire response of the uninsulated steel specimens in tests 1 through 3.

Figures J–9 through J–12 show comparisons of the modeled and measured temperatures and heat fluxes for tests 3 (2.0 MW heptanes/toluene fire) and test 5 (3.0 MW heptanes fire). The agreement for the highest temperatures is excellent. Analysis of both the model and the thermocouple measurements is under way to determine the source of their differences at the lower temperatures, especially in test 5. The spikes in the heat flux plots are artifacts—the result of the periodic nitrogen blasts to reduce soot accumulation on the gage surface.

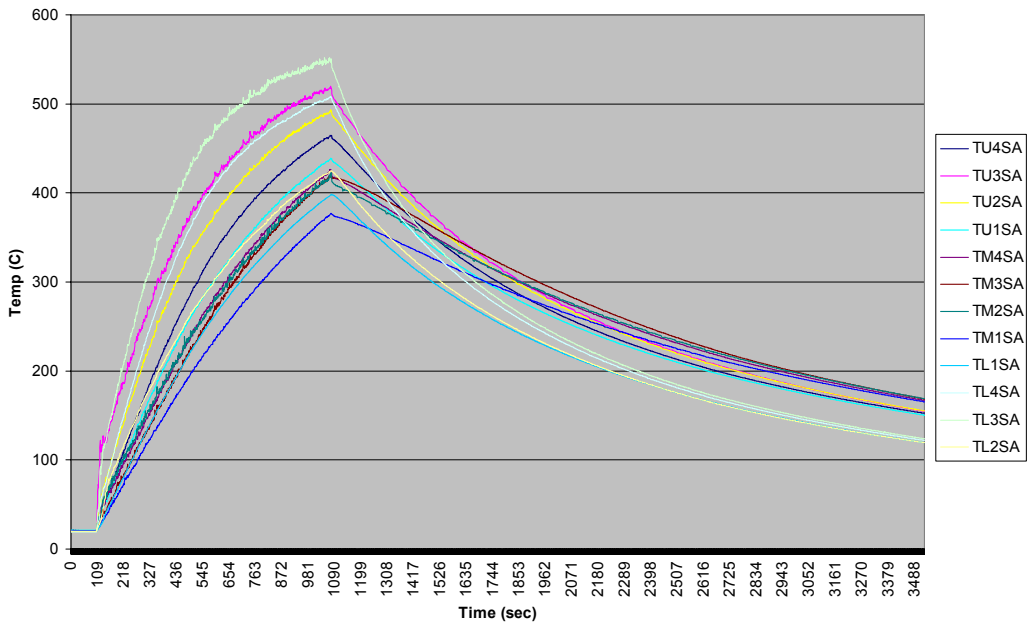

Figure J–8. Temperature-time history for truss A in test 3.

While the data analysis is not yet complete, the following are valuable preliminary observations:

- The prediction of the upper layer temperatures was within experimental uncertainty. Since the heat flux to the walls and objects within the upper layer is highly dependent on the upper layer temperature, these predictions were also accurate.The prediction of the time for the steel surfaces to reach 600 °C was accurate.

- The sootier burning fuel led to similar temperature rise in the ceiling and the steel above the fire plume.

- The model predicted the asymmetric shape of the fire plume, caused by obstructions to uniform flow through the compartment.

Further analysis will use Smokeview for visual comparison of the test results and the model predictions. This will determine how well FDS captures both the fire phenomena and the thermal patterns in the compartment. Quantitative analysis of the data will then determine the numerical accuracy of the predictions. Similar analysis will be performed to determine the accuracy of the finite element modeling of the thermal patterns within the bare and insulated steel components.

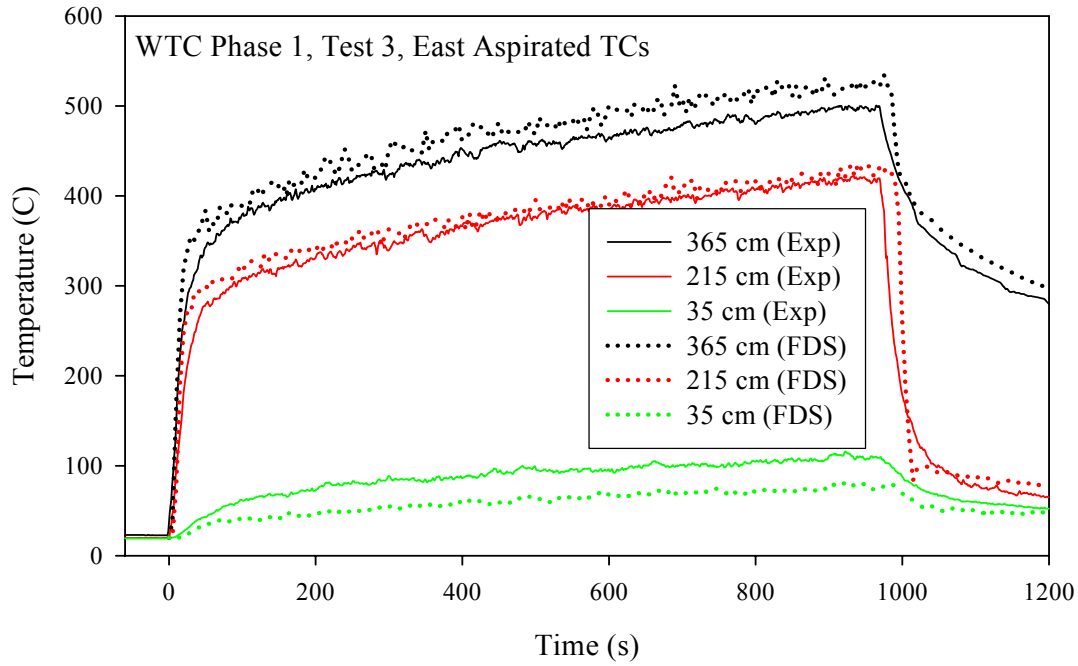

Figure J–9. Comparison of gas temperatures, test 3, exhaust side of compartment.

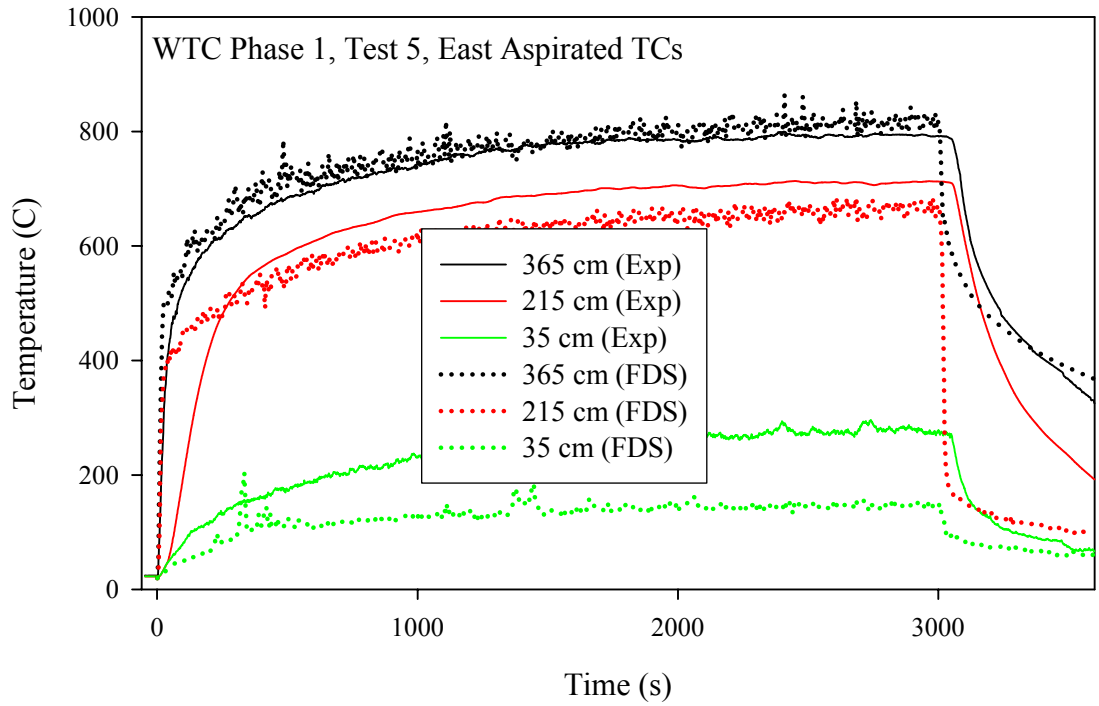

Figure J–10. Comparison of gas temperatures, test 5, exhaust side of compartment.

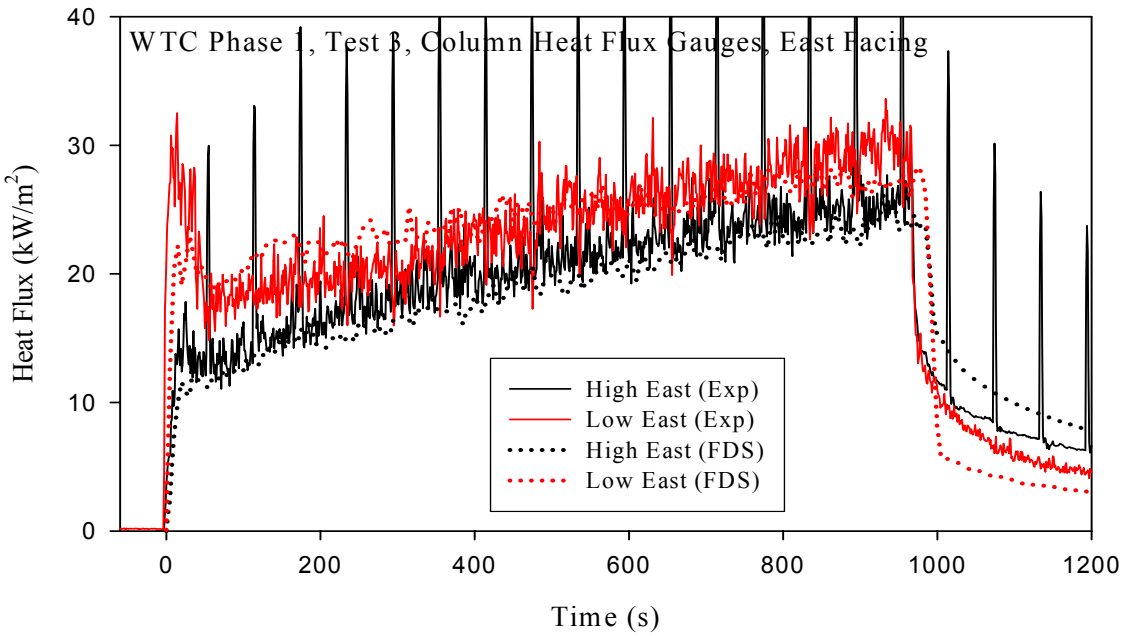

Figure J–11. Comparison of heat fluxes to column, test 3.

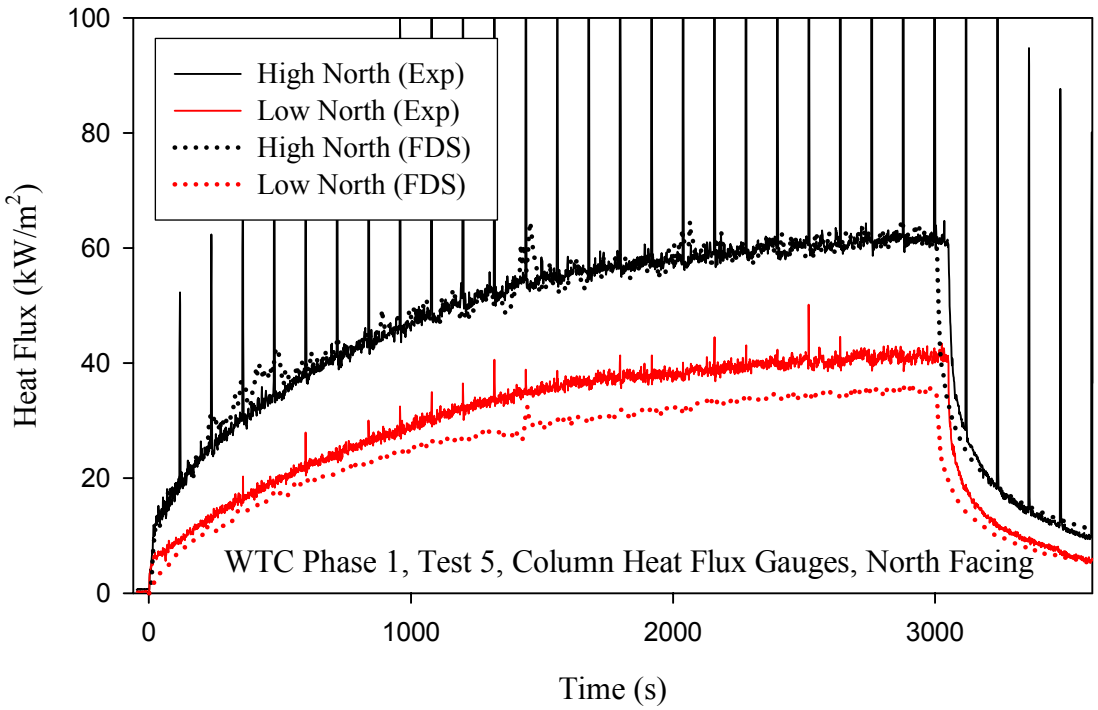

Figure J–12. Comparison of heat fluxes to column, test 5.

J.3 EXPERIMENTS FOR GUIDING THE FDS FIRE GROWTH PREDICTIONS

In the early stages of this Investigation, the FDS combustion module was enhanced to enable the inclusion of charring materials, such as those that comprise much of the office furniture. Thermophysical property data from the combustion of small (100 mm × 100 mm) samples of the furnishings were obtained using the Cone Calorimeter. These data became input to the fire simulation. A set of real-scale experiments was then designed and performed (July and August 2003) to identify any need for further enhancements to the fire model. In each of these experiments, a single workstation (i.e., an office cubical or module), similar to those in the WTC offices, was burned under a hood. A soffitted ceiling allowed for the collection of hot fire effluent and the accordant thermal radiation to the test specimen. Some of the tests examined the effects on the burning rate of jet fuel and/or noncombustible material occluding a fraction of the workstation surfaces.

J.3.1 Description of the Experiments

Materials

Workstations come in a variety of styles and finishes. However, they tend toward similar size and mass. They are also fabricated of materials with similar burning behavior, e.g., the work surfaces are generally laminated particleboard or wood. Most of the workstations burned here were of a single generic type. For comparison, one high-end unit (identical to those in the aircraft impact floors in WTC 1) was also burned in a manner identical to one of the tests of the generic units.

The generic workstation examined is shown photographically in Figs. J–13 and J–14. The layout, including the placement of the various nonstationary items, was suggested by personnel from a company that supplied office furnishings to the occupants of WTC 1. Information on the distribution of papers and other office items was provided by a frequent visitor to these offices. The workstation covered a footprint nominally 2.44 m × 2.44 m (8 ft × 8 ft) and was surrounded by privacy panels.

- The panels were 1.22 m (4 ft) high, except that on one side the panel was 1.52 m (5 ft) tall and supported a bookcase. On the side opposite the bookcase, there was a 1.22 m (4 ft) wide open entrance opening. The panels were made of a steel and softwood frame, covered on both sides with layers of fiberglass padding and perforated steel and a thermoplastic cover fabric. A few sheets of copier paper were tacked to the cubicle walls on three sides.

- The work surfaces were formed from four sections of laminated medium density fiberboard supported by steel brackets from the wall panels. Four document boxes contained a total of four reams of copier paper. Additional paper was stacked horizontally on the desk surface.

- The seat and back of the office chair were a nonthermoplastic fabric over polyurethane foam supported by a one-piece thermoplastic shell; its five-legged base was thermoplastic with steel framing and support elements.

Figure J–13. Photograph of right side of generic workstation.

Figure J–14. Photograph of left side of generic workstation.

- The three file cabinets (0.91 m wide, 0.51 m deep, 0.68 m high [36 in. × 20 in. × 27 in.], with two horizontal drawers) were painted steel; they rested directly on the carpet. Two of the cabinets contained two reams each of copier paper as a rough means of assessing the extent to which paper in file drawers might contribute to a fire.

- The bookcase (1.22 m [48 in.] long) had a steel shelf and top but these were supported only on their ends by combustible end panels; the steel front closure panel was fabric-covered steel and it was open (on top of the bookcase). Ten document boxes held about 13 reams of copier paper.

- The carpet tiles were nylon fiber-faced over a dense foam rubber backing. A square area 2.74 m × 2.74 m (9 ft × 9 ft) was covered with 36 carpet tiles.

- The computer monitor was a nominally 17 in. CRT-based unit. Its front face was taped with fiberglass tape and it was pointed toward the wall panel opposite the cubicle opening for safety in the event of an implosion. The keyboard was placed in its normal location, parallel to the sloped segment of the work surface. The computer processor (tower-type container with plastic only on the front face of the container) was placed on the floor next to a waste paper basket (both on the side opposite the cubicle opening).

- The wastebasket was thermoplastic and contained one ream of copier paper atop five balled-up paper ream wrappers.

Thermophysical characterizations of six of the generic workstation materials (carpet, panels, work surface, chair seat, paper stack, and computer monitor shell) were obtained using the Cone Calorimeter. These data were to serve as input to FDS. Since the physical behavior of at least some of the work station materials (and the objects from which they were taken) was expected to be more complex than was revealed in the Cone tests, it was anticipated that these full-scale tests would provide clues as to necessary empirical adjustments in the FDS predictions.

The high-end unit was similar to the generic workstation, with the principal differences being:

- The wall panel construction was somewhat different having a 3 mm (0.125 in) layer of flame-retarded polyester fiber beneath the outer fabric, a more open steel panel beneath this, a central fiberboard layer (3 mm thick) and an all steel peripheral frame (no wood). The fiberboard roughly doubled the amount of woody fuel within the wall panels of the enclosure and put it into a much higher surface area form in which it could be expected to burn appreciably faster. It should be noted, however, that this increase in woody fuel was only about 10 percent to 15 percent of the total available in the desk surfaces. Also, its enclosure deep within the wall panels delays its burning.

- The file cabinets (four, with a total face length of 2.67 m rather than three with a total face length of 2.44 m) had a flammable, charring plastic surface on the drawer fronts that added 15 percent to 20 percent of flammable area.

The chair was constructed somewhat differently (seat and back as separate pieces) and behaved as if its upholstered surfaces were flame-retarded. The high-end workstation is shown in Fig. J–15.

Figure J–15. Photographs of high-end workstation.

Test Configuration and Instrumentation

The workstation to be tested was placed on top of a double layer of 13 mm (1/2 in) thick calcium silicate sheets. These in turn rested on a set of four weighing cells, one at each corner. Each workstation (including furnishings) weighed approximately 730 kg (1,600 lb) and contained approximately 300 kg (660 lb) of combustible material. The weighing cells are accurate to ±0.1 kg (0.2 lb). The entire assembly was placed beneath the hood of the NIST 10 MW calorimeter hood to allow continuous heat release rate measurement.

A fire typically forms a layer of hot, smoky combustion products near the ceiling of a room. Thermal radiation from this layer plays a significant role in fire spread. Thus the test fixture included partitions to hold the combustion products from these test fires. The ceiling was a 3.66 m × 3.66 m (12 ft × 12 ft) section of 13 mm thick calcium silicate board. It was supported on a water-cooled steel frame 2.74 m (9 ft) above the floor of the workstation. To keep the gases from flowing quickly across the ceiling and thus not forming an appropriate layer, the ceiling was surrounded on all four sides by a steel skirt that draped down 0.61 m (2 ft) from the ceiling.

The test instrumentation included:

- Instrumentation in the hood exhaust duct for measurement of rate of heat release.
- Four video cameras placed to record the progression of flame spread over the objects in the cubicle. Their view of the combustibles became observed by the wall panels and the flames themselves as the fire grew in intensity. An observer narrated the fire growth to supplement what the cameras recorded directly.
- In two tests, an upward-facing, water-cooled Schmidt-Boelter total heat flux gage 127 mm (5 in) above the cubicle floor, near the cubicle center.
- An external total heat flux gage mounted so as to view the entire fire from one side. This provided a signal that was proportional to the instantaneous HRR of the fire and was useful for certain timing issues.
- In two tests, six 24-gage chromel/alumel thermocouples to follow the progress of the fire on the underside of the desk surfaces.

Ignition Scenario

The initiation of the tests was in keeping with the workstation being one of a large array on a given floor of a large office space and a fire propagating through the array. Thus a large ignition source (a 2 MW, four-nozzle spray burner over a 2 m × 1 m pan) was placed immediately adjacent to the exterior of one wall panel of the test station, simulating the burning of the adjacent workstation. The size and placement (pan bottom 0.81 m above the floor) of this ignition source were guided by preliminary FDS predictions.

The igniter fire was supported by a flow of commercial-grade liquid heptanes (mixed isomers) sprayed at a nominally steady rate from the four nozzles pointing downward toward the pan. The heptane mix was supplied from a reservoir by a variable-speed pump. The desired fuel flow was preset before the test and measured in triplicate by catching the flow from each nozzle in a volumetric cylinder for a typical period of 20 s. The nominally 2 MW fire supported by the heptane flow typically impinged almost continually on the ceiling above the igniter. There was thus an essentially continuous wall of flames radiating toward the workstation along the central three-fourths of the length of one panel. In addition, the workstation was subject to radiation from the hot ceiling and the hot smoke captured below the ceiling.

Test Variables

There are numerous variables that might influence the burning of a workstation such as that examined here, starting with the nature of the materials and their spatial arrangement, the ignition conditions, etc. There are also variables unique to the WTC fires: the amount of paper-based clutter in a workstation, the possible presence of jet fuel (and its amount), the possible presence and amount of inert rubble generated by the airplane impact (fallen ceiling tiles, inert dust from pulverized concrete and/or wallboard), varying degrees of impact-induced break-up and compaction of the work station itself, and presence of combustible solids from the airplane.

The tests were designed keeping the purposes in mind: (a) identify the current capability of FDS to predict complex burning behavior using combustion data from small-scale specimens and (b) obtain clues to improving the combustion algorithm should the predictions be of insufficient accuracy. Thus the two selected variables were those that could affect the workstation fires in manners that test FDS and are important in the WTC context: the presence or absence of both jet fuel and of inert rubble. The inert rubble was taken to be representative of fallen ceiling tiles.

The primary test set thus focused on two levels of two variables examined in a full factorial design. This calls for four tests: (1) no inert rubble and no jet fuel, (2) rubble but no jet fuel, (3) jet fuel but no rubble and (4) rubble and jet fuel. The levels of the two variables were estimated to produce differences in burning behavior that would be clearly observable. Thus the inert rubble was chosen to cover approximately 30 percent of the horizontal surfaces facing the hot ceiling. As performed, 24 of the 40 ceiling tiles were on the horizontal desk surfaces; 14 were on the central, open floor area; and 2 were on the chair seat. The fraction of the plan view horizontal area covered by these tiles was approximately 31 percent. A total of 4 L (approximately 1 gal) of Jet A was spread over these same horizontal surfaces.[1]

Two additional tests were conducted. The first test (in the entire series) utilized what was nominally one-half of a generic workstation, though it included both a full chair and full computer. This was done to gage the burning behavior of what was an entirely unknown system. The fourth test was of the high-end workstation. Both of these were conducted with no jet fuel and no inert rubble present.

Test Procedure

The workstation was assembled a few hours before a test. Since the ambient humidity was high (approximately 70 percent) for most of the tests, the paper was covered with plastic sheeting if it was to be exposed for more than 2 hours, although this probably did not preclude significant moisture pick-up in the outer portions of the paper piles. That moisture would be expected to somewhat slow the ignition process relative to a more normal humidity of 50 percent.

At the beginning of each test, all instruments were calibrated. [The heat release rate was also measured for a few minutes after the test ended in order to verify the calorimeter baseline.] The heptanes flow was measured in triplicate. The test was initiated by starting the heptanes flow and immediately igniting it with a torch. This defined time zero. The heptanes flow was left on until late in the test unless there was

[1] Areas close to the impact could have been drenched with higher quantities. The workstations would also have had to be extensively fragmented, which is not a situation being examined here. Another pragmatic factor that kept the jet fuel loading down was the probability that higher levels would have pushed the calorimeter beyond its maximum allowable capacity.

an indication that the fire was going to significantly exceed the 10 MW calorimeter capacity; this happened only once (test 5). The full test was video taped by all four cameras and a narration was fed to one camera, describing the sequence of ignition events that spread the fire over the accessible flammable surfaces. In two cases (tests 3 and 4) the residual weight of the paper piles in the two file drawers was obtained as a measure of the participation of this paper in the overall fire.

In the two tests in which jet fuel was placed on the horizontal surfaces prior to the start of a test, this was done just before ignition of the 2 MW spray burner. A sprinkling can was used in two separate operations, each involving 2 L of the liquid fuel. First, the liquid was sprinkled on the horizontal desk surfaces and the objects on them (i.e., the various paper stacks or document boxes, the computer monitor and the keyboard) using a timed movement that attempted to allot an equal amount of liquid to each one-third section of the total work surface. The desk surface had been leveled after installation so that the liquid would not run preferentially in one direction. Next, an equal amount of the liquid was sprinkled in a similarly timed manner on the central open section of the carpet (not under the desk surfaces). Since the chair occupied a portion of this space, the allotment for that portion went onto the chair seat and back surfaces. For the objects on or in contact with the desk surface, there was some tendency for the jet fuel to wick into them if they were porous. This was true of the paper, the inert tiles and the wall panel fabric just above the desk surface.

J.3.2 Preliminary Results

Figures J–16 and J–17 show the workstation early in a test and at a time just before the peak heat release was reached. Figures J–18 through J–23 show the heat release rate curves from the six fire tests.

Figure J–16. Photograph of workstation soon after ignition in test 2.

Figure J–17. Photograph of workstation near the peak heat release rate in test 2.

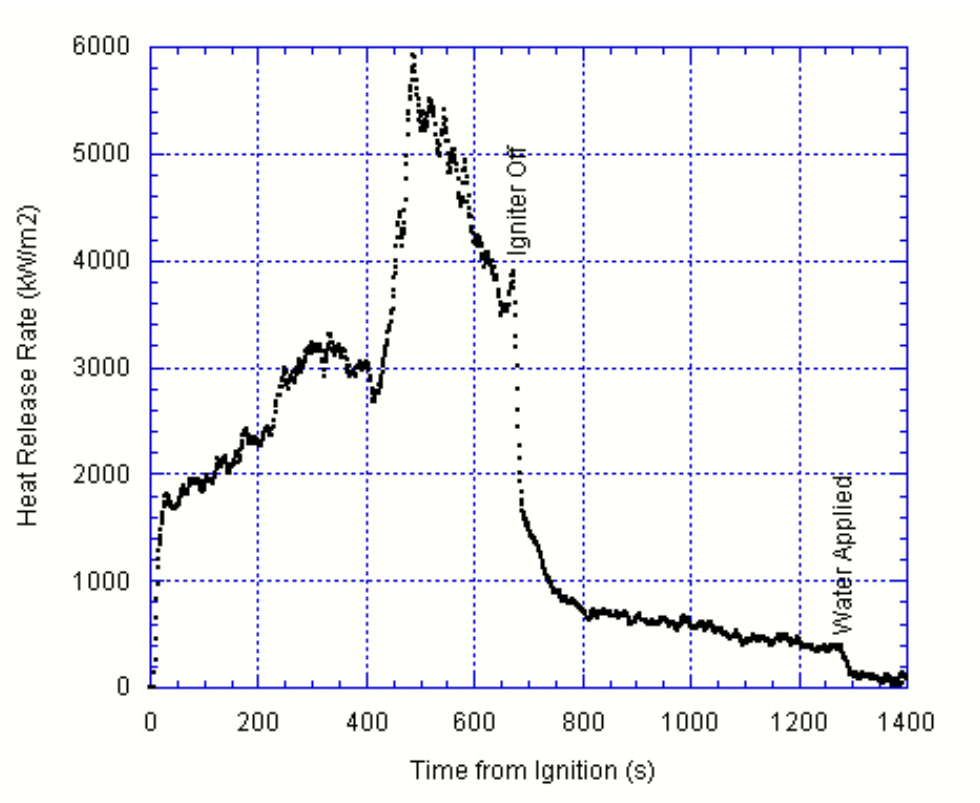

Figure J–18. Heat release rate versus time for single workstation test 1.

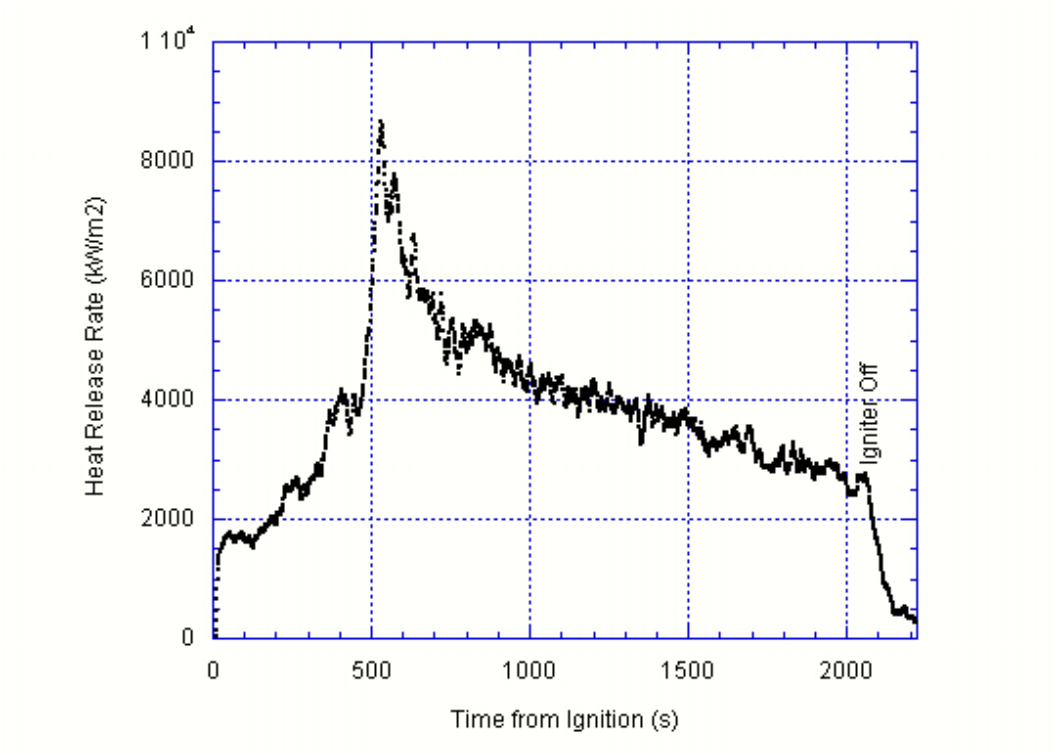

Figure J–19. Heat release rate versus time for single workstation test 2.

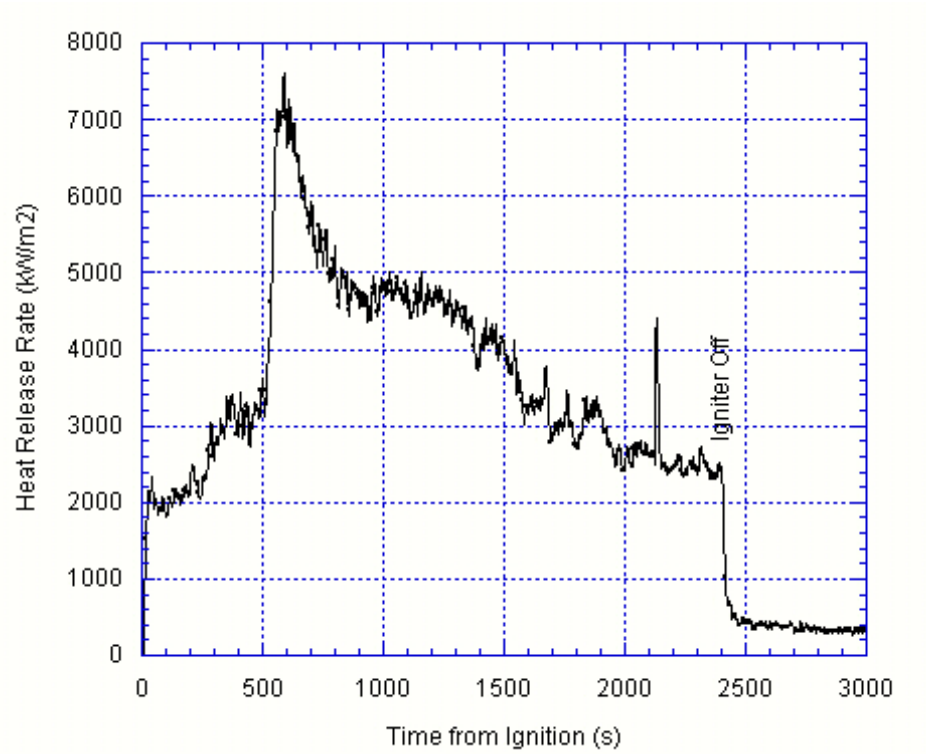

Figure J–20. Heat release rate versus time for single workstation test 3.

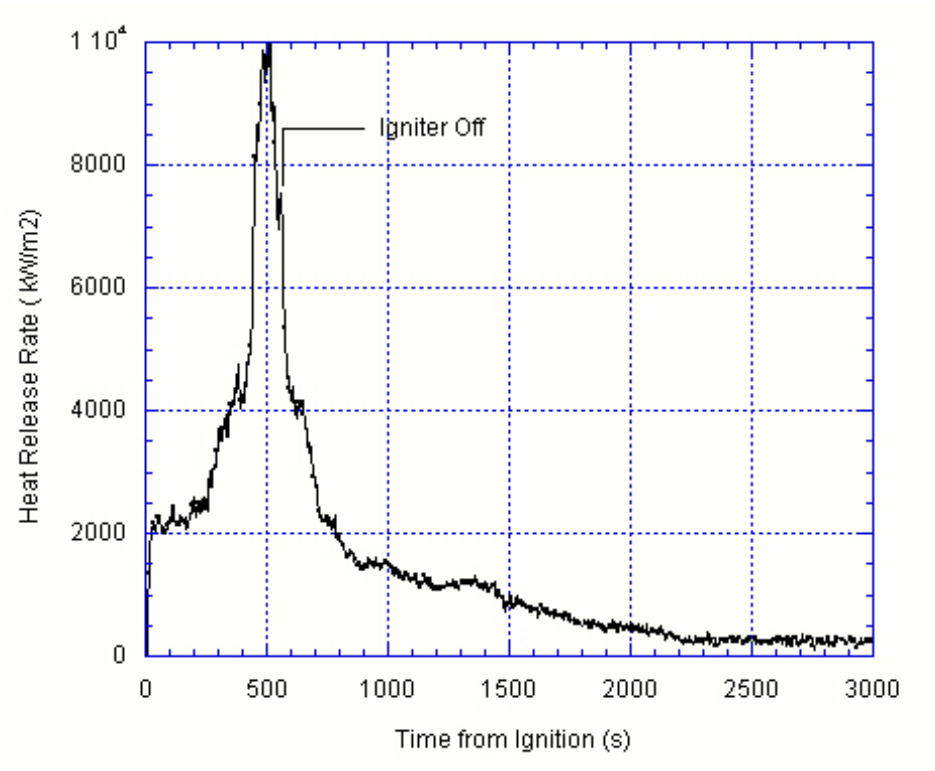

Figure J–21. Heat release rate versus time for single workstation test 4.

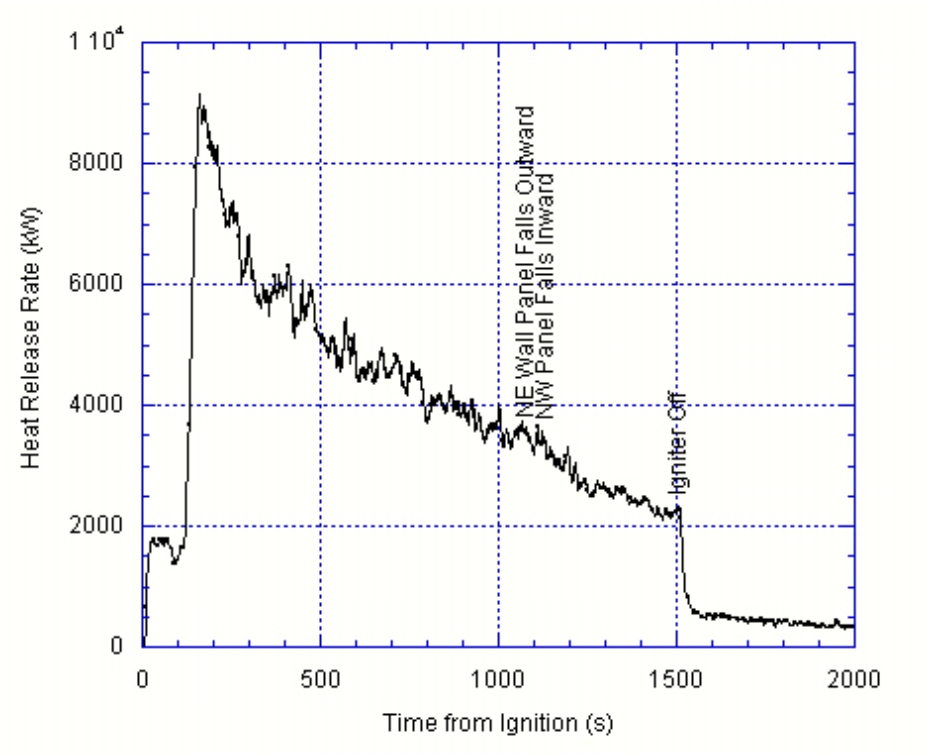

Figure J–22. Heat release rate versus time for single workstation test 5.

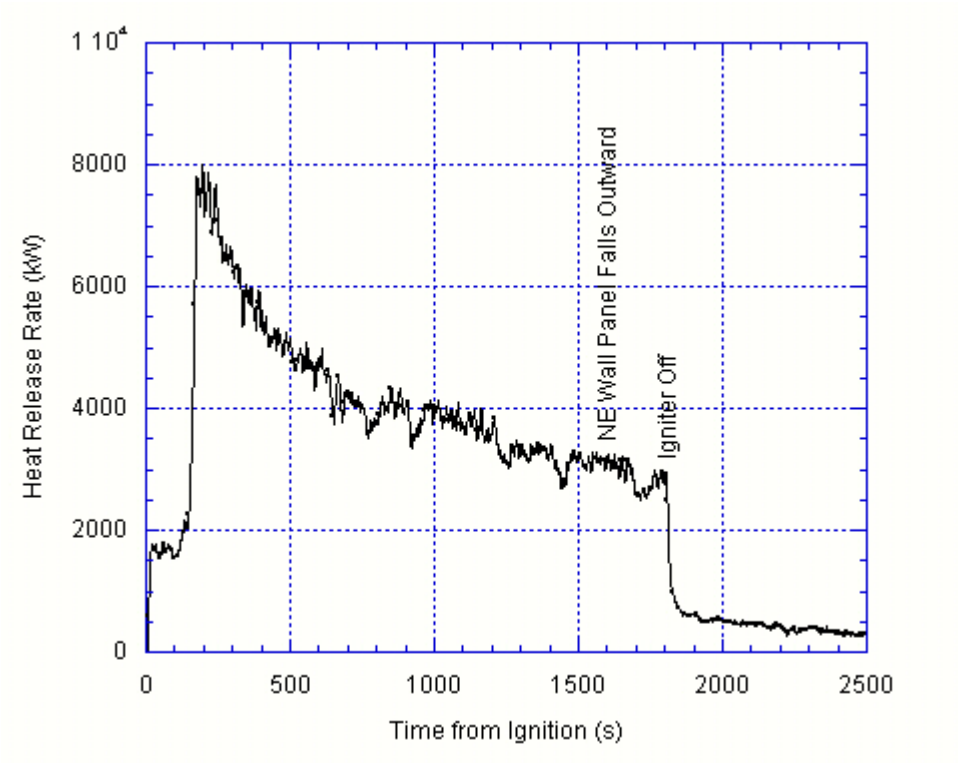

Figure J–23. Heat release rate versus time for single workstation test 6.

Table J–3 lists the peak HRR values from each test plus the time to that peak, rounded to the nearest 10 s. The HRR peak is given in two ways: first, as the absolute highest single reading recorded (for a 1 s interval) and second, as the average of the value at this peak plus values up to 5 s to either side of this peak. The latter compensates for both noise in the calorimeter system and in the fire itself; it is doubtful that objects in a real room can respond in any meaningful way to small HRR fluctuations in a fire that is under 10 s in duration. The averaged values are about 3 percent lower than the absolute peak values, a result of the sharpness of the peaks in every case.

Table J–3. Peak heat release rates and times to peak.

Test	Test Specimen	Jet Fuel (Yes/No)	Inert Tiles (Yes/No)	Peak HRR (kW)	Time to Peak HRR (s)
1	Half of generic workstation	N	N	5920/5770	490
2	Generic work station	N	N	8700/8480	530
3	Generic work station	N	Y	7560/7300	590
5	Generic work station	Y	N	9120/8910	160
4	High-end work station	N	N	9890/9660	510
6	Generic work station	Y	Y	7960/7690	200

The videotapes of the fires show that the peak HRR corresponds closely to simultaneous burning of all the “accessible” combustible surfaces in the workstation interior. This included the top of the desk surface, the objects on it, the exposed area of the materials in the bookcase, the full chair area (but see below), the exposed area of the carpet (i.e., not that under the three steel file cabinets), objects on the

carpet (computer processor case and wastebasket) and the underside of the desk, except above the steel file cabinets where the air access was limited. The interior surfaces of the wall panels contributed negligibly because the thermoplastic fabric melted and rolled downward into a mass having much less surface area than the original fabric prior to igniting. This type of behavior is not captured in Cone Calorimeter tests.

The following observations emerge from comparison of the results in Table J–3:

- The peak fire intensity from the half workstation is about two-thirds that of the full workstation. This is probably primarily the result of two factors:
  - The same chair was present in both cases; this chair has an estimated HRR peak in the neighborhood of 1/2 MW by itself.
  - The inert steel file cabinets cover twice as much of the carpet in the second half of the workstation, precluding its participation in the HRR peak; this lowers the HRR contribution from the second half of the workstation.
- The computer was also totally combusted within the first half of the experiments, though this was a substantially lesser heat source than was the chair.
- The ceiling tiles reduced the peak HRR in proportion to their coverage of the burning surfaces; both just under 15 percent. While there was 30 percent coverage of the upward facing horizontal surfaces, there was no coverage of the underside of the desk, the carpeting below the desk or the underside and back of the chair. As noted above, all of these were burning at the peak. (The reduction might become more than linear if nearly all of the upward facing horizontal surfaces were covered since this could preclude the progressive flame spread that gets all accessible surfaces involved)
- The principal effect of the presence of 4 L of Jet A on the horizontal surfaces was in shortening the time to involvement of all accessible combustible surfaces, and thus the time to the peak HRR. The peak itself was boosted upward only about 5 percent, presumably because the Jet A helped boost the overall fuel gasification rate somewhat while adding its high heat of combustion. When the inert tiles were also present, the Jet A was poured across their top surfaces temporarily rendering these surfaces flammable. Since the tiles were porous, the Jet A burning rate on them was reduced, however, and the tiles still managed to produce a 13 percent to 14 percent reduction in the peak HRR relative to the case with Jet A and no tiles.

From examination of the videotapes and the commentary, NIST determined that, when there was no Jet A present, there was a fairly reproducible progression of ignition events leading up to the HRR peak:

- The onset of the igniter fire bathed the entire workstation in radiant heat.
- The igniter fire was not the pilot flame that ignited other objects, although FDS simulations suggest that the peak fluxes on surfaces facing the igniter were of the order of 30 kW/m^2 or more, well above the minimum flux for piloted ignition of the various exposed surfaces. Even the top of the computer monitor shell, which gasified extensively only 20 cm from the spray burner

flames, did not appear to ever have directly been ignited by those flames. Instead the progression of flaming was initiated by the top sheets on the paper stacks. Its presence in many places made it highly instrumental in spreading the flames to the computer monitor shell, the desktop and the top of the chair back. Flaming material from the chair fell onto the carpet, igniting it. Subsequent spread on the carpet was delayed, however, until the chair was fully involved, along with the remainder of the upward-facing surfaces of the desktop. Later, paper ignition brought flames to the two other sides of the desk area in the workstation.

- Once the entire area at and above the top of the desk surface was burning, the "compartment" under the desk flashed over from the radiant heat from the upper compartment and especially the heat from the burning chair. With all flammable surfaces ignited, the HRR quickly peaked. The specific construction of the chair and its location were critical to this fire growth process:

  - One corner of the seat was deliberately placed to extend approximately 15 cm under the desk surface on which the computer keyboard rested. This assured that some heat would reach this space early on, even though the chair flames would contact the relatively ignition resistant underside of the desk.

  - When only the upholstered surfaces of its seat and back were burning, the chair retained its original shape, and little of its heat reached the lower compartment area.

  - When the thermoplastic support shell of the chair began to melt and flow to the floor, extensive heat flowed directly into the "compartment" under the desk.

  - The partial steel skeleton kept the chair from collapsing and maintained burning from desk level to floor level. The flame radiation to the cavity under the desk quickly ignited the materials located there, while the upper part of the chair flames played on the desk, assisting ignition of its underside.

Since chairs of different designs (and thus different burning behavior) could be fabricated from the same materials, the detailed fire behavior of the chair cannot be inferred simply from the Cone Calorimeter data for the component materials. Thus, empirical treatment of its HRR process is necessary.

As expected, the progression of ignition events in the presence of Jet A was different. Ignition of the materials in the cubicle occurred more quickly. However, the manner of the acceleration was not what might have been expected.

- Since the flash point of Jet A is at least 46 °C (approximately 20 °C above the ambient temperature), initially there would be no flammable mixture of vapors above the liquid fuel surface. As the strong radiant flux from the spray burner bathes the workstation, the videos show an increasingly dense aerosol rising from the various wetted surfaces near the spray burner. These did not ignite, as evidently turbulent mixing of the vapor plume above the surfaces quickly diluted the fuel vapor below the lean flammable limit. Instead, in the first Jet A test, a random piece of flaming material rose from the burner area and drifted down on top of the desk, immediately igniting the Jet A. In the second test, a flaming piece of debris from the burner landed on top of the bookcase where there was no jet fuel and it had no effect. The paper stacks

on the work surface next to the spray burner finally dried out, began to char, and then transitioned into flaming, igniting the jet fuel.

- The Jet A flames then spread rapidly, but did not sweep continuously around the desktop. Presumably the initial evaporation period left some dry spots that stopped the spread.

- The carpet was ignited by flaming matter dropping from the chair. Apparently the turbulent vapor plume dilution process mentioned above prevented the flames from jumping downward to the carpet from the flaming desk surface, even though the carpet was emitting an aerosol. At any rate, the subsequent flame spread on the carpet was rapid.

- None of these steps is resolved in the HRR curves of Figs. J–21 and J–22 due to the rapidity with which the curves jumped rapidly to their peak values soon after the Jet A ignited. As in the "dry" tests, the peak corresponds to all accessible combustible surfaces burning simultaneously.

The rapid decay in HRR after the peaks in all tests presumably reflects several factors that should be captured in the combustion algorithm in FDS:

- The various paper piles developed a thick ash layer that would drive down their burning rate.

- Char formation on the desk surfaces drove down its burning rate.

- The carpet began to burn out.

However, a number of geometric changes occurred that are beyond the capability of FDS to reproduce:

- The chair fire rapidly collapsed to a pool fire on the floor whose reduced burning area meant a reduced HRR.

- The front of the bookcase, resting on top of that unit, typically fell, changing the location of its 13 reams of paper.

- The desk surface bowed progressively as it charred through, and then it collapsed, with separate sections doing so at differing times. The initial desk collapse probably did not greatly affect its burning rate, but ultimately what was left was a complex rubble pile whose burning would not be predictable from any knowledge of the original configuration coupled with Cone Calorimeter data.

- The wall panels collapsed at random times, both inward and outward, typically rather late in the fire.

Thus, the further one goes out on the HRR curve, past the peak, the less it is predictable by an FDS calculation that retains the original geometry. Fortunately, the major effects appear to occur well after the desk surfaces collapse and the time when contiguous workstations would become ignited and dominate the heat release.

Numerical grids of 10, 20, and 40 cm were used to model the fires and ensure that the model was not sensitive to grid cell size. Figure J–24 shows a preliminary comparison of the FDS HRR prediction with the measured values for test 2 (no jet fuel, no inert tiles). The quality of fit is typical of the test series.

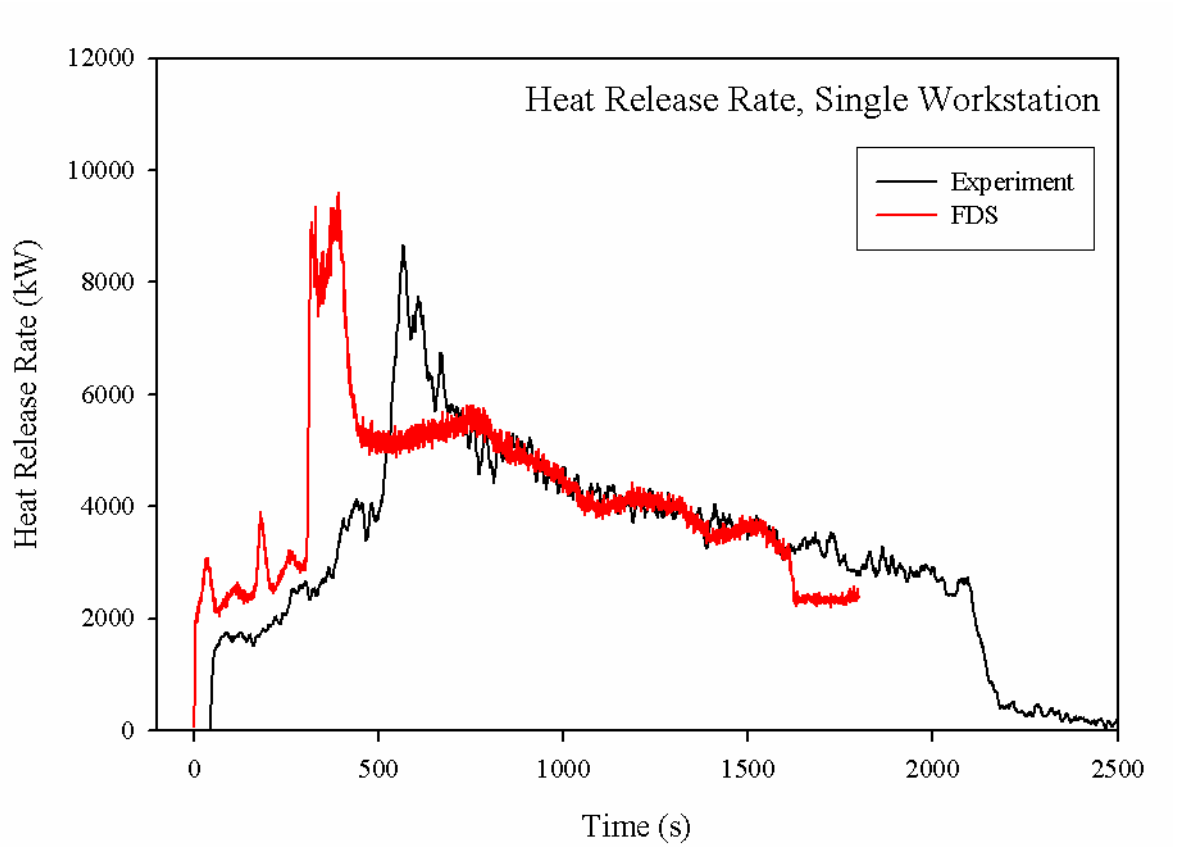

Figure J–24. Preliminary comparison of predicted and measured HRR values.

For these simulations, the thermal properties of the major materials making up the workstations were derived from Cone Calorimeter experiments. The carpet and privacy panel were modeled as thermoplastics, that is, the burning rate was assumed to be proportional to the heat flux from the surrounding gases. The desk was modeled as a charring solid, in which a pyrolysis front propagates through the material leaving a layer of char behind that insulates the material and reduces the burning rate. Details of the pyrolysis models can be found in the *FDS Technical Reference Guide* (McGrattan et al. 2002). Each feature of the experimental curve was related (using annotations made during the tests and from the video tapes) to specific aspects of the workstation combustion.

There are similarities and discrepancies between the experimental data and this prediction.

- The shape and magnitude of the two curves is encouragingly similar, as is the total heat release (area under the curves).
- The peak HRR occurred sooner in the simulation. In the experiment, the time to peak HRR was strongly influenced by the melting of the chair plastic onto the carpet. As noted above, this level of detail is not captured in the numerical model.

- At long times, the simulation drops to the residual HRR of the 2 MW burner somewhat more abruptly than does the experimental curve, indicating that it has run out of combustible mass sooner. The importance of this effect is modest, given the geometric changes during the test (listed above) and the similarity of the total heat released.

A more complete analysis will be detailed in the forthcoming documentation report.

J.4 EXPERIMENTS FOR FIRE MODEL VALIDATION

Following the experiments described above and the accordant improvements in FDS, a series of large-scale experiments was conducted in the NIST Large Fire Laboratory between November 4 and December 10, 2003. The six experiments were designed to assess the accuracy with which FDS predicts the fire spread, heat release rate, and thermal environment in a compartment burning multiple workstations in a configuration characteristic of that found in the WTC buildings. In each of these experiments, sets of three workstations, identical to the generic ones tested in Section J.3, were burned in a large compartment (see Fig. J−25). The challenges to the model included varying the location of the ignition burner (and thus the fire ventilation), adding jet fuel and/or noncombustible material occluding a fraction of the workstations' surfaces, and "rubblizing" the workstations. FDS simulation of each test was carried out before the test was conducted.

The steel-frame experimental enclosure was 10.8 m long × 7.0 m wide × 3.4 m tall (35.5 ft × 23 ft × 11 ft) and was lined with three layers of 13 mm (0.5 in) calcium silicate board (see Fig. J−26). There was a subfloor (not included in the above dimensions) to house instrumentation. The enclosure had openings on the front mimicking window openings through which fresh air entered and heat and combustion products were emitted. The narrowed openings limited the amount of fresh air that entered the burning enclosure.

Each of three workstations was placed on an isolated platform made of calcium silicate board. The top surface of each platform was flush with the floor of the compartment. Each platform was supported on water-cooled load cells, located in the subfloor, to monitor the mass of the workstation throughout the test. The load cells were the same as those described in Section J.3.

Two of the workstations were contiguous, exemplifying a part of the type of cluster that exists in many large office spaces. The third workstation was separated from the other two by an aisle, representing a part of a second cluster. This array was to enable assessment of FDS's ability to replicate two different modes of cubicle-to-cubicle fire spread: direct flame impingement and radiative ignition from the hot ceiling layer.

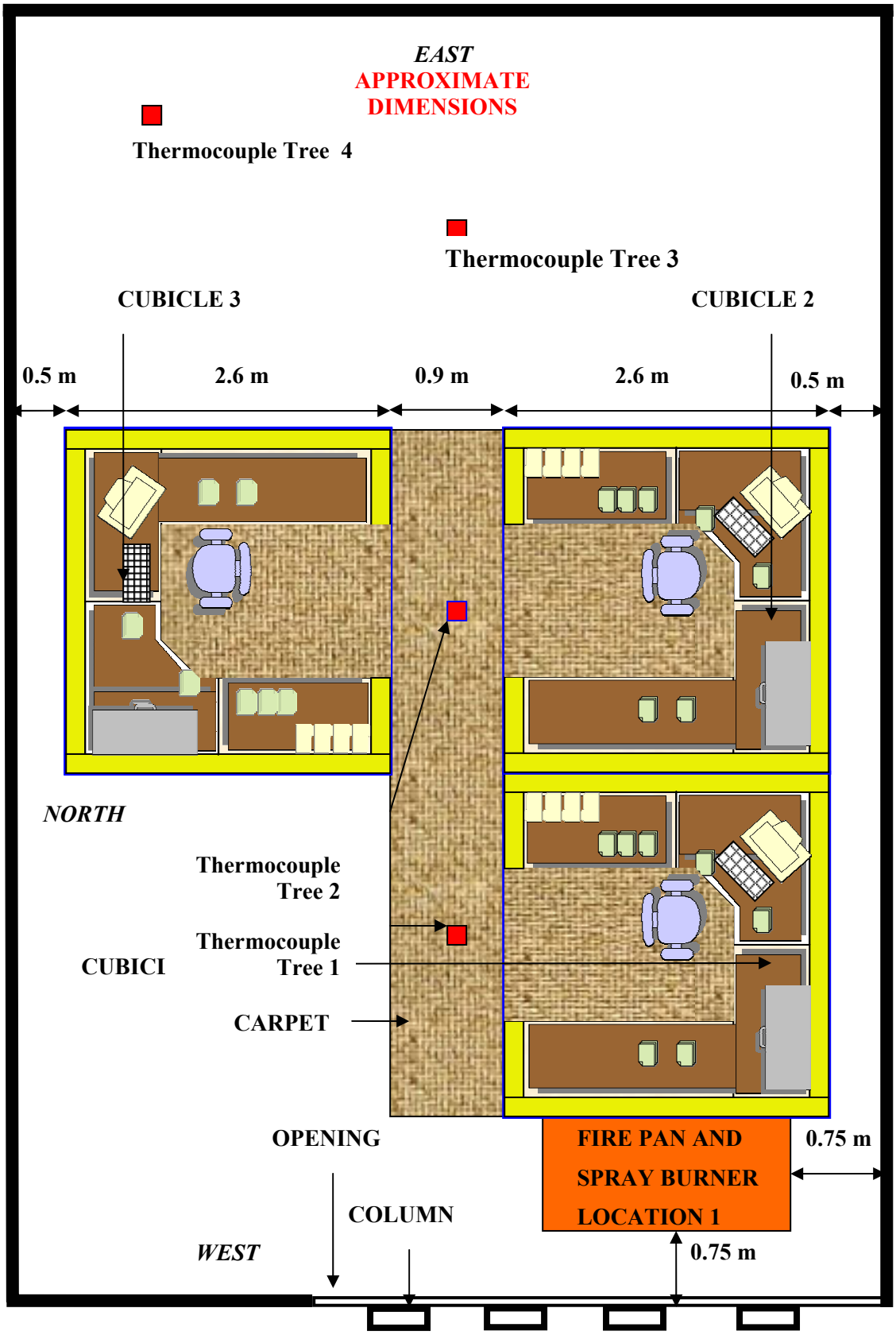

Figure J–25. Plan view of test configuration.

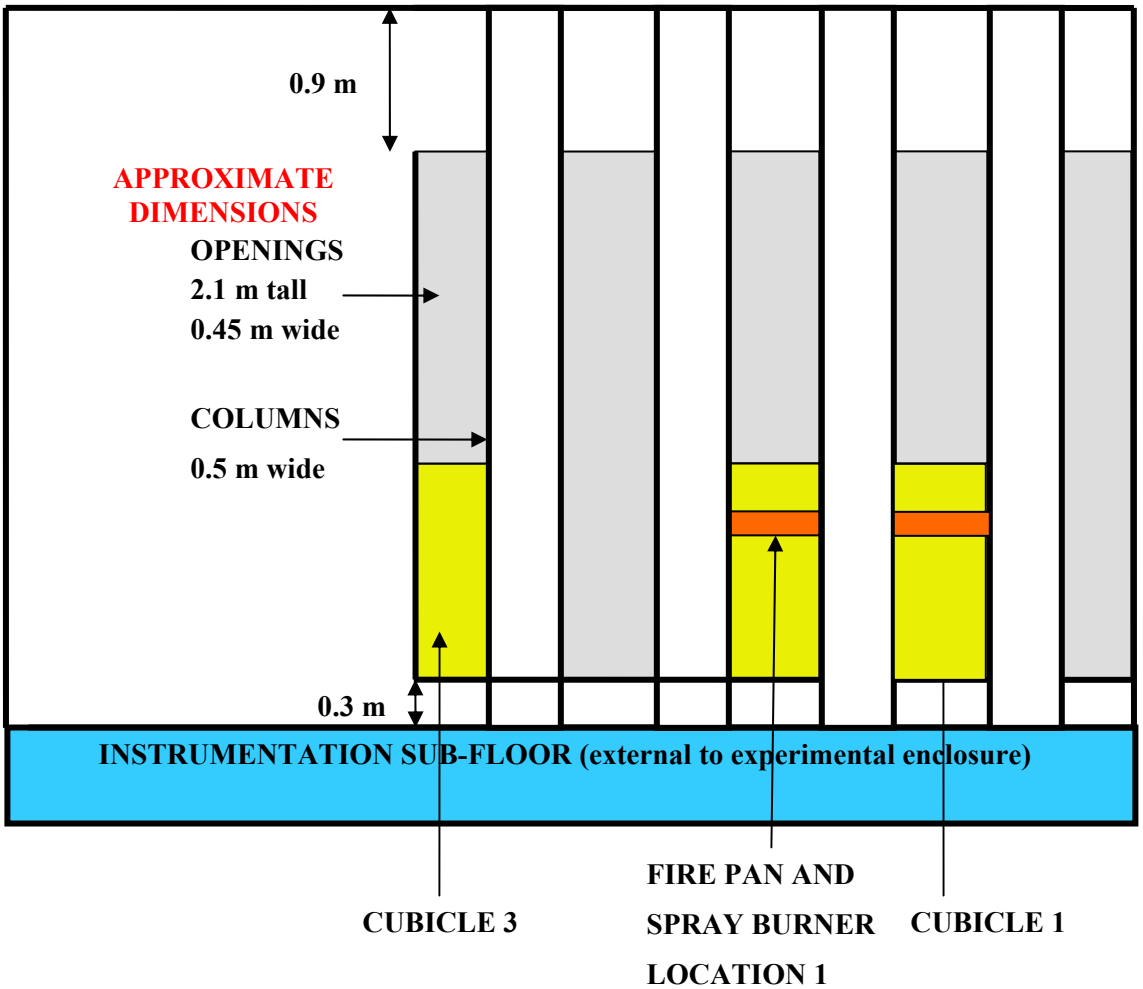

Figure J–26. Elevation view of test configuration.

The west end of the enclosure was located under a 10 m × 12 m hood for collection of the effluent and measurement of the heat release rate.

Other instrumentation included:

- Four floor-to-ceiling trees of thermocouples to measure vertical profiles of temperature(see Fig. J−27);
- Thermocouples on the desk surfaces to track flame spread;
- Two downward-facing, water-cooled Schmidt-Boelter total heat flux gages in the ceiling to measure radiative heat flux;
- Two water-cooled Schmidt-Boelter total heat flux gages mounted on the west wall; and
- Four video cameras placed to record the progression of flame spread over the objects in the cubicle.

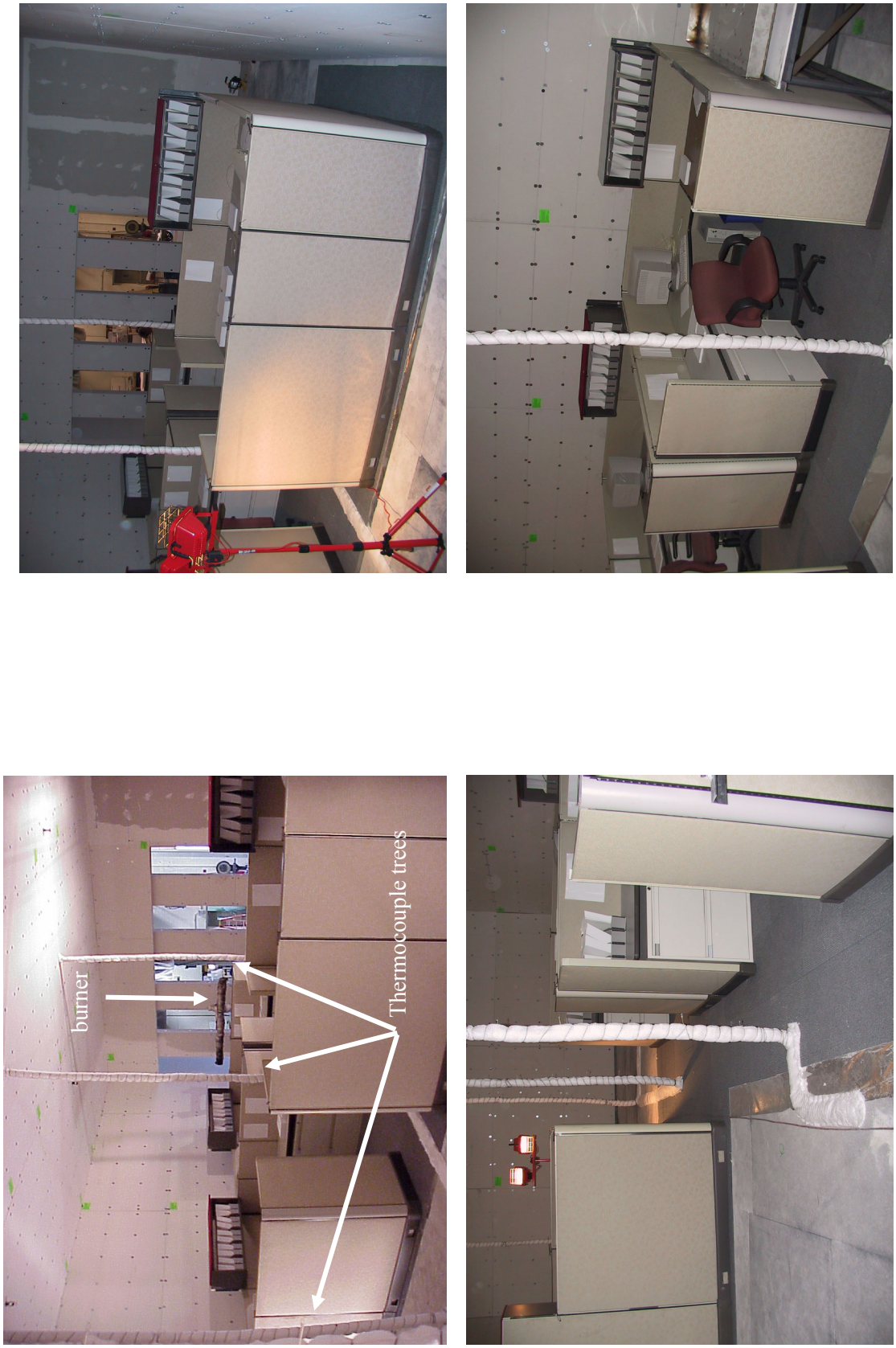

Figure J–27. Views of interior of test fixture.

The liquid spray burner, pan, and fuel (mixture of heptanes) were the same as used in the Section J.3 experiments. Depending on the test, the burner was located abutting the top of a workstation partition at the east end of cubicle 1 or the west end of cubicle 2. The ignition fire intensity was a nominal 2 MW fire. The spray burner was operated for the first few minutes of the tests, for either 2 min or 10 min depending on the test scenario.

Materials

The workstations were of the same type as the generic units used in the experiments reported in Section J.3. The carpet tiles, which covered the floor of the cubicles and the aisle, were also the same type used in experiments reported in Section J.3.

Test Variables

The experimental matrix is shown in Table J–4. The experiments investigated the impact of several parameters on the fire behavior:

Table J–4. Test matrix.

Test	Ceiling Tiles	Jet Fuel	Burner Location	Workstations	Windows
1	None	None	Front	Intact	No
2	None	None	Front	Intact	No
3	Present	Present	Front	Intact	No
4	Present	None	Rear	Intact	No
5	Present	Present	Rear	“Rubble”	No
6	None	Present	Rear	Intact	Yes

- Location of the burner. This was placed either abutting the west end of cubicle 1 or abutting the east end of cubicle 2. These two sites resulted in significantly different access to the air needed for combustion. In the former (“front”) location, much of the oxygen in the air initially entering the enclosure was consumed by the burner and the burning cubicle 1, with the result that limited oxygen was available for combustion in the middle and rear of the compartment. With the burner in the latter (“rear”) location, the fresh air passed directly to the rear of the compartment.

- The application of 12 L of jet fuel evenly distributed about each workstation. The procedure was the same as used in the experiments reported in Section J.3.The presence of fallen ceiling tiles. Having seen the effect of coverage of 30 percent of the top surfaces in the previous test series, NIST covered approximately 70 percent of the top surfaces here.

- Fractured furniture. In one experiment (test 5), NIST investigated the effect of different degrees of “rubblizing” the furniture.

    - In cubicle 1, the workstation pieces were placed unassembled on top of each other, occupying the same footprint as the assembled workstation. The same mass of combustibles was present as in the fully assembled cubicle tests. No steel filling cabinets were used. Ceiling tiles and broken up drywall were intermixed with the rubble.

- Cubicle 2 was the same as cubicle 1, except without the drywall.
- For cubicle 3, the workstation was partially assembled. The same mass of ceiling tile and drywall as in cubicle 1 were intermixed with the cubicle components.
- Window breakage. Test 6 had four glass windows mounted on the north end of the west wall. During the course of the fires in the WTC towers, a number of windows were broken, presumably by the heat from the fires. These result in a change in both the degree and pattern of ventilation.

Test Procedure

This was similar to that followed in the experiments reported in Section J.3, except that the ignition burner was turned off after approximately 2 min for tests 3, 5, and 6 (when jet fuel was present) and for 10 min for Tests 1, 2, and 4. The tests continued until the HRR fell below 0.5 MW, which was typically 60 min after ignition.

J.4.1 Preliminary Results

Figures J–28 and J–29 show the east view of the compartment before and during a test, respectively. A few observations about the tests were:

- The peak HRR was approximately 11 MW for four of the tests. In test 5, the peak value was only approximately 6 MW. In test 6, the peak HRR reached almost 16 MW.
- As in the single workstation tests, the peak value was reached earlier when jet fuel was present.

Figure J–30 shows how the enclosure was represented in FDS. The computational grid size was 0.4 m (1.3 ft) on a side. Note that the chair, computer monitor, and paper have been collected together into "boxes" with comparable mass to the various items that were spread throughout the workstations. To the right are five windows that are similar in size to those of WTC 1 and WTC 2.

The preliminary plot in Fig. J–31 depicts the degree to which the heat release rate measurements agreed with those predicted by FDS.

The overall degree of agreement between the model and the experimental data is quite good, despite some modest local differences. In the analysis leading to candidate improvements in the modeling, it is important to maintain perspective of the effect of these differences on the accuracy needed in reconstructing the actual WTC fires. For fires that are sufficiently severe that they threaten the structural integrity of the building, many such workstations will be burning concurrently. These workstations will be at various stages of their combustion. Thus, for example, features occurring at long times in Fig. J–31 may not merit closer replication, while those features occurring at short times (and thus have a bearing on the ease of fire spread among workstations) may merit attention.

Figure J–28. View of fire compartment before the start of test 6.

Figure J–29. View of fire compartment 2 minutes after the start of test 6.

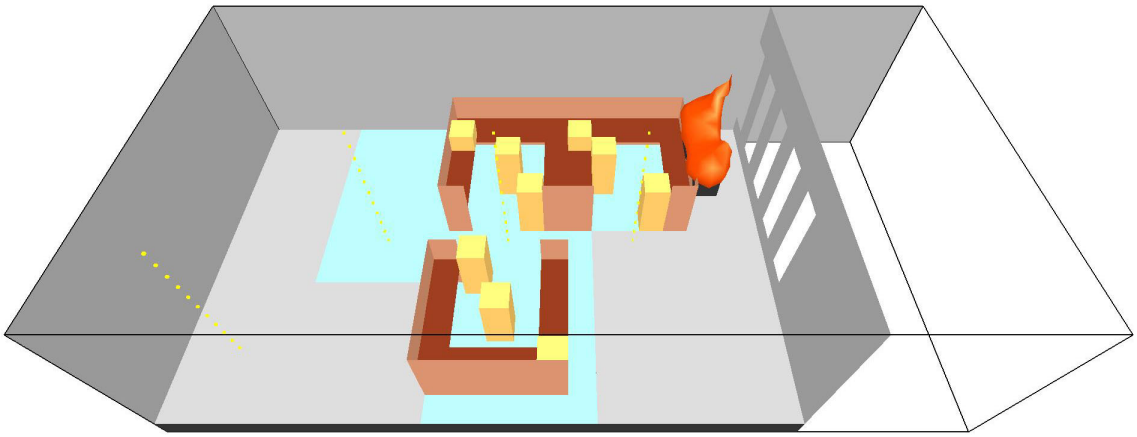

Figure J–30. Fire Dynamics Simulator 3D rendition of experimental enclosure.

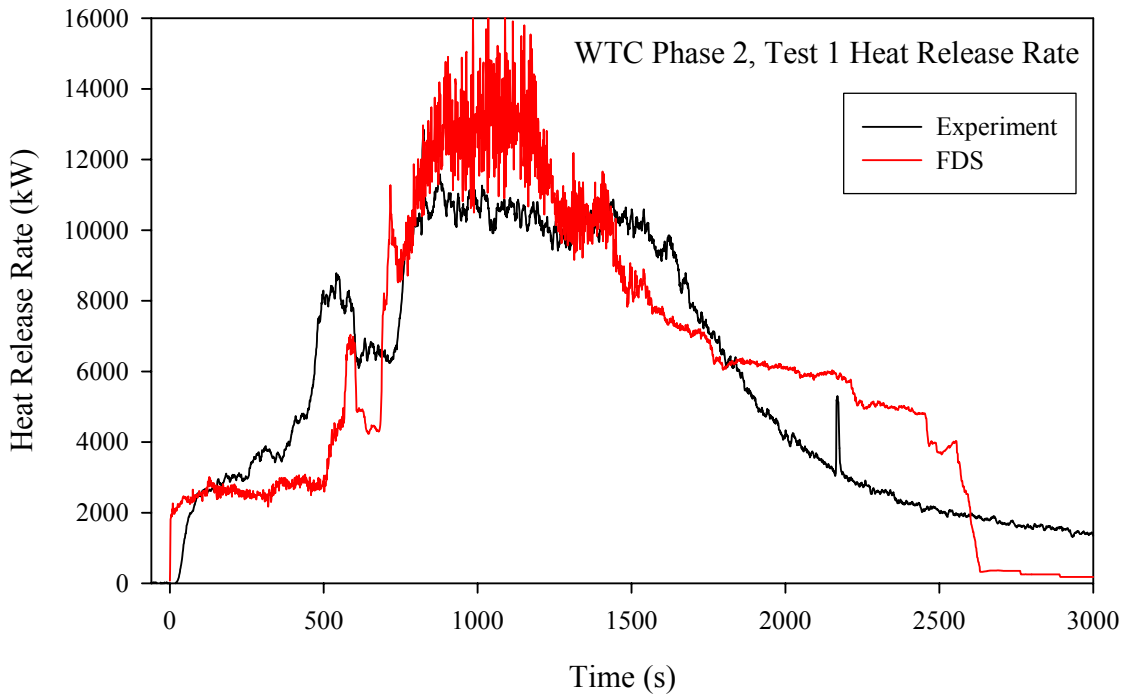

Figure J–31. Comparison of measured and predicted heat release rate for test 1.

J.5 REFERENCES

McGrattan, K.B., H.R. Baum, R.G. Rehm, G.P. Forney, J.E. Floyd, K. Prasad and S. Hostikka. 2002. Fire Dynamics Simulator (Version 3), Technical Reference Guide. NISTIR 6783. National Institute of Standards and Technology, Gaithersburg, MD.

Attachment 1
Simulating the Fires in the World Trade Center

1.1 INTRODUCTION

In the months following the attacks on the World Trade Center (WTC) and the Pentagon, there was an active debate in the fire protection engineering community about the fires that erupted following the impact of the aircraft on the buildings. Because fires of this magnitude in these types of buildings are rare, there is a wide spectrum of opinion about the fire temperatures and their effect on the structural steel. Much of the fire literature consists of empirical correlations derived from experiments ranging from bench scale to room scale. Extrapolating these well-known correlations to the WTC requires a reexamination of the underlying assumptions. Many of these correlations are appropriate for a narrow range of fire sizes and building geometries, and cannot be directly applied to the WTC fire scenarios. As a result, computer fire models that have been developed over the past decade are being applied to the analysis.

As part of the investigation, the National Institute of Standards and Technology (NIST) has conducted simulations of the fires in each building using a computational fluid dynamics (CFD) model known as the Fire Dynamics Simulator (FDS). This attachment will describe the experiments conducted at NIST to calibrate and validate the FDS model for use in the WTC project, and it will describe the techniques developed to simulate the very extensive fires that spread over 6 to 12 floors in the different buildings.

1.1.1 Experimental Program

Two large-scale test series were conducted to provide validation for the FDS, plus various small-scale experiments were conducted to provide the model with input data for different materials. The large-scale test programs are referred to as Phase 1 and Phase 2. Both test series involved fires in compartments with the same ceiling height as a floor in WTC 1 or WTC 2. Phase 1 was a series of fire tests with a liquid fuel spray burner generating a fixed amount of energy in a compartment with various targets and obstructions, like columns, trusses and other steel objects. These tests were designed to test the accuracy of the model, and its sensitivity to changes in various input parameters. Phase 2 was a series of fire tests in which office workstations similar to those used in WTC 1, WTC 2, and WTC 7 were burned in a compartment with limited openings to simulate the under-ventilated conditions of the WTC fires. These tests were designed to test the model's ability to characterize the burning behavior of real furnishings under conditions typical of the WTC fires. Only the Phase 2 work will be discussed in this attachment.

1.1.2 NIST Fire Dynamics Simulator

FDS is a CFD model of fire-driven fluid flow. It solves numerically a form of the Navier-Stokes equations appropriate for low-speed, thermally-driven flow with an emphasis on smoke and heat transport from fires (McGrattan et al. 2002). Version 1 was publicly released in February 2000. The core algorithm is an explicit predictor-corrector scheme, second order accurate in space and time. Turbulence is treated by means of the Smagorinsky form of Large Eddy Simulation (LES). For most applications,

FDS uses a mixture fraction combustion model. The mixture fraction is a conserved scalar quantity that is defined as the fraction of gas at a given point in the flow field that originated as fuel. The model assumes that combustion is mixing-controlled, and that the reaction of fuel and oxygen is infinitely fast. The mass fractions of all of the major reactants and products can be derived from the mixture fraction by means of "state relations," empirical expressions arrived at by a combination of simplified analysis and measurement.

Radiative heat transfer is included in the model via the solution of the radiation transport equation for a non-scattering gray gas, and in some limited cases using a wide band model. The equation is solved using a technique similar to finite volume methods for convective transport; thus the name given to it is the Finite Volume Method (FVM). Using approximately 100 discrete angles, the finite volume solver requires about 15 percent of the total CPU time of a calculation, a modest cost given the complexity of radiation heat transfer. FDS approximates the governing equations on a rectilinear grid. The user prescribes rectangular obstructions that are forced to conform with the underlying grid.

All solid surfaces are assigned thermal boundary conditions, plus information about the burning behavior of the material. Usually, material properties are stored in a database and invoked by name by the user. An extensive effort was undertaken to characterize the thermal properties of common items found in an office setting, like privacy panels, stacks of paper, computer monitors, office chairs, pressboard tables, desks, and carpeting. These materials will be described next.

1.2 CALIBRATION AND VALIDATION EXPERIMENTS

The experimental program concentrated on the thermal properties of the office furnishings that constituted the bulk of the combustible fuel within the WTC buildings under study. Several types of office workstations typical of those used in WTC 1 and WTC 2 were purchased at area office supply stores. The thermal properties of the major materials making up the workstations were derived from cone calorimeter experiments. These properties were input into FDS, which was used to simulate the burning behavior of a single workstation burning under a 2.5 m ceiling with baffles to contain a hot layer of smoke above the burning workstation. Other than the baffled ceiling, no walls surrounded the workstation other than its own privacy panels. The thermal properties of the workstation components were adjusted slightly so that the FDS prediction of the heat release rate would match the experiment. Then the model was used to predict the heat release rate of 3 workstations burning within a large enclosure. The purpose of this exercise was to determine if FDS could simulate the dynamics of a fire in a setting similar to WTC 1, WTC 2, and WTC 7.

1.2.1 Description of the Workstation Components

Cone calorimeter experiments at three different heat fluxes were performed for the carpet, desk (wood), computer monitor, chair, privacy panel, and stacked paper. For the simulations of the WTC fires, only the carpet, desk and privacy panel data were used directly. The carpet and privacy panel were modeled as thermoplastics, that is, the burning rate is assumed to be proportional to the heat flux from the surrounding gases. The desk was modeled as a charring solid, in which a pyrolysis front propagates through the material leaving a layer of char behind that insulates the material and reduces the burning rate. Details of the pyrolysis models can be found in the FDS Technical Reference Guide (McGrattan et al. 2002).

The desk was modeled as a charring solid. The thermal properties of the wood and its char were taken from both the calorimeter experiments and the work of Ritchie et al. (1997). It is 2.8 cm thick with density 450 kg/m^3, specific heat 1.2 kJ/kg/K at 20 °C and 1.6 kJ/kg/K at 900 °C, conductivity 0.13 W/m/K at 20 °C and 0.16 W/m/K at 900 °C. The ignition temperature is 360 °C and the heat of combustion is 14,000 kJ/kg ± 800 kJ/kg. Its total available energy content is 210 MJ/m^2 ± 50 MJ/m^2.

The carpet was modeled as a thermoplastic with density 750 kg/m^3, specific heat 4.5 kJ/kg/K, conductivity 0.16 W/m/K, ignition temperature 290 °C, thickness 6 mm, heat of vaporization 2,000 kJ/kg, heat of combustion 22,300 kJ/kg ± 600 kJ/kg, and total available energy content 61 MJ/m^2 ± 2 MJ/m^2.

The privacy panel was modeled as a thermally-thin thermoplastic. The product of specific heat, thickness and density is 0.73 kJ/m^2/K. Its surface density is 0.25 kg/m^2, ignition temperature 380 °C, heat of vaporization 6,000 kJ/kg, heat of combustion 30,000 kJ/kg ± 500 kJ/kg. Its total available energy content is 6.0 MJ/m^2 ± 1.3 MJ/ m^2.

The test compartment walls and ceiling were made of three layers of 1.27 cm (0.5 in) thick Marinite I, a product of BNZ Materials, Inc. (http://www.bnzmaterials.com).[2] The manufacturer provided the thermal properties of the material used in the calculation. The density is 737 kg/m^3, conductivity 0.12 W/m/K. The specific heat ranged from 1.2 kJ/kg/K at 93 °C to 1.4 kJ/kg/K at 425 °C.

In the simulations of the fires within the WTC, the chair, computer, paper, and other miscellaneous items within the workstation were modeled as a single item by lumping the mass together into large "boxes" and distributing them throughout the workstation. It is common practice in fire protection engineering to use surrogate materials for fire experiments, and this practice has been extended to numerical modeling. Over the years, various items have been developed that are representative of various types of commodities. For example, wood cribs are often used to represent ordinary combustibles found in residential or light industrial settings. Paper cartons with various amounts of plastic within are also used as surrogates for a wide range of retail commodities. One in particular is called the FMRC (Factory Mutual Research Corp.) Standard Plastic Commodity, or more commonly, Group A Plastic. This test fuel is often used in sprinkler approval testing at Factory Mutual and Underwriters Laboratories in the US, and similar test fuels have been developed in Europe. In the late 1990s, FDS was used to simulate large scale rack storage fires to determine the effectiveness of the combined use of sprinklers, roof vents and draft curtains (curtain boards). As part of this effort, a considerable amount of work was done to characterize the thermal properties of Group A Plastic (Hamins and McGrattan 2003). Because Group A Plastic has been shown to be fairly representative of fires fueled by a mixture of paper (cellulosic materials) and plastic, and because it has been used in numerous FDS simulations, it was decided to model the contents of the office workstations with a fuel similar to Group A Plastic. Blind predictions of the single open workstation burns were made using the material properties obtained during the sprinkler/roof vent study, and then these properties were adjusted to match the results of the experiments. Thus, the single workstation burns served to calibrate the model. They were not intended to be validation experiments. The validation experiments consisted of burning 3 workstations at a time in an under-ventilated compartment.

[2] Certain commercial equipment, instruments, or materials are identified in this document. Such identification does not imply recommendation or endorsement by the National Institute of Standards and Technology, nor does it imply that the products identified are necessarily the best available for the purpose.

The surrogate fuel is modeled as a homogenous solid whose density is 172 kg/m^3. The paper carton is treated as a thermally-thin material whose density × specific heat × thickness is 1.0 kJ/m^2/K. Its ignition temperature is 370 °C and the heat of combustion is 30,000 kJ/kg. The heat release rate of the boxes ramps up to 450 kW/m^2 in about 1 min. Note that this fuel package is similar, but not the same, as Group A Plastic. The density has been increased to account for all the miscellaneous items within the workstation. Also note that unlike the desk, partition and carpet, the boxes are simply given a burning rate rather than a heat of vaporization, meaning that the boxes will burn at the given rate regardless of the heat flux upon them as long as the surface temperature remains above its ignition temperature. The reason for this is that it is not possible to predict the burning rate using the heat feedback approach because the geometry of the scattered fuel is too complex to directly predict the response of the material to the thermal insult. By collecting all the scattered items into boxes, the geometry of the combustibles is greatly simplified, and as a result the burning behavior must be simplified as well.

1.2.2 Description of the Simulations

The geometry of the compartment is relatively simple. The overall enclosure is rectangular, as are the vents and most of the obstructions. Numerical grids of 20 and 40 cm were used to model the fires. The purpose of the grid variation was to ensure that the model was not sensitive to the change in grid cell size. Typically, enclosures of this size are modeled using 10 cm grid cells. However, for the simulations of WTC 1, WTC 2, and WTC 7, a 40 cm grid was used. By simulating the experiments at 20 cm and 40 cm, NIST can test if the model produces significantly different results with grid cells of different sizes. Figure 1–1 is a snapshot of a simulation showing the fire and the major geometric features of the compartment for the simulations. Note that the surrogate fuel packages are placed roughly where the computer monitor, chair and paper were located. Six tests were performed, with various ignitor locations and fuel arrangements. A 2 MW burner was pl aced either near the windows of the compartment overlooking the workstation nearest the openings in Tests 1, 2, and 3. The burner was placed towards the rear of the compartment overlooking the workstation in the rear of the compartment in Tests 4, 5, and 6. In Tests 3, 5, and 6 Jet A fuel was poured over the workstations and surrounding carpet. To simulate this in the model, spray nozzles were positioned over the center of each workstation, 2 m above the floor. These nozzles are normally used to simulate water sprinklers, but in this case, the water was replaced by a liquid having similar properties to Jet A. The nozzles were activated for 2 s, in which time the equivalent amount of liquid as in the tests was ejected and spread over the furnishings.

In Test 5, Workstations 1 and 2 were disassembled prior to the burn and the contents were piled on top of the respective load cells. To model this scenario, the burning rate of the collective fuel packages was reduced by one half to account for the decrease in burning area of the fuel pile. The choice of one half was somewhat ad hoc. No free burns of workstation parts had been performed. This was the only test in which the simulated fuel packages had to be modified from their free-burn values. In this regard, Test 5 was used to calibrate, not validate, the model.

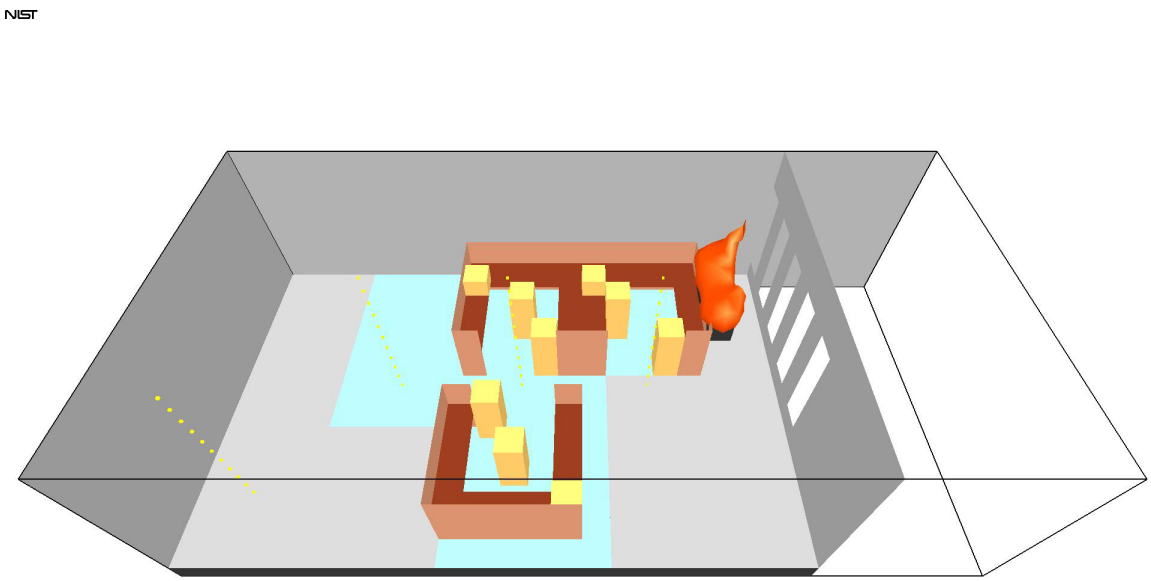

Figure 1–1. Geometry of the Phase 2 simulations.

From a modeling perspective, the objective of the simulations of the Phase 2 experiments was to demonstrate that a simplified model of an office workstation can be used to predict the burning behavior of a group of workstations in an enclosure with features similar to WTC 1, WTC 2, and WTC 7. Because of the magnitude of the simulations of the building fires, the model of the workstation had to be fairly crude. However, because of the many uncertainties in the initial conditions of the fire simulations, the lack of detail in the model is not considered to be a problem. The model fires had similar growth patterns, peak heat release rates, decay patterns, and compartment temperatures.

The model also captured the major features of the individual tests. For example, Tests 1 and 4 were similar in design except for the burner location. In Test 1 the burner was near the windows; in Test 4 it was near the rear of the compartment. The peak heat release rate was reached in about 15 min in Test 1, whereas it was reached in about 10 min in Test 4. The model shows a similar trend. The faster growth of Test 4 is probably due to the fact that the compartment heated up more quickly with the fire deep inside rather than near the windows, leading to more rapid spread of the fire across the pre-heated furnishings. Even though ceiling tiles were distributed over the desk and carpet in Test 4, this did not seem to have a noticeable effect on the growth, or at the very least the burner position seemed to have a far greater role in explaining the difference between Tests 1 and 4. The comparison of HRR between model and experiment is shown for Test 1 in Figs. 1–2. The upper layer temperature in the rear of the compartment for this same test is shown in Figs.1–3. The results for the other tests are comparable. The peak HRR and temperature are predicted well, as well as the duration of the fires. Both the peak values and the duration of the burning are important for the WTC simulations because it is not only important to predict the temperatures that the structural steel was exposed to, but also the duration of the exposure.

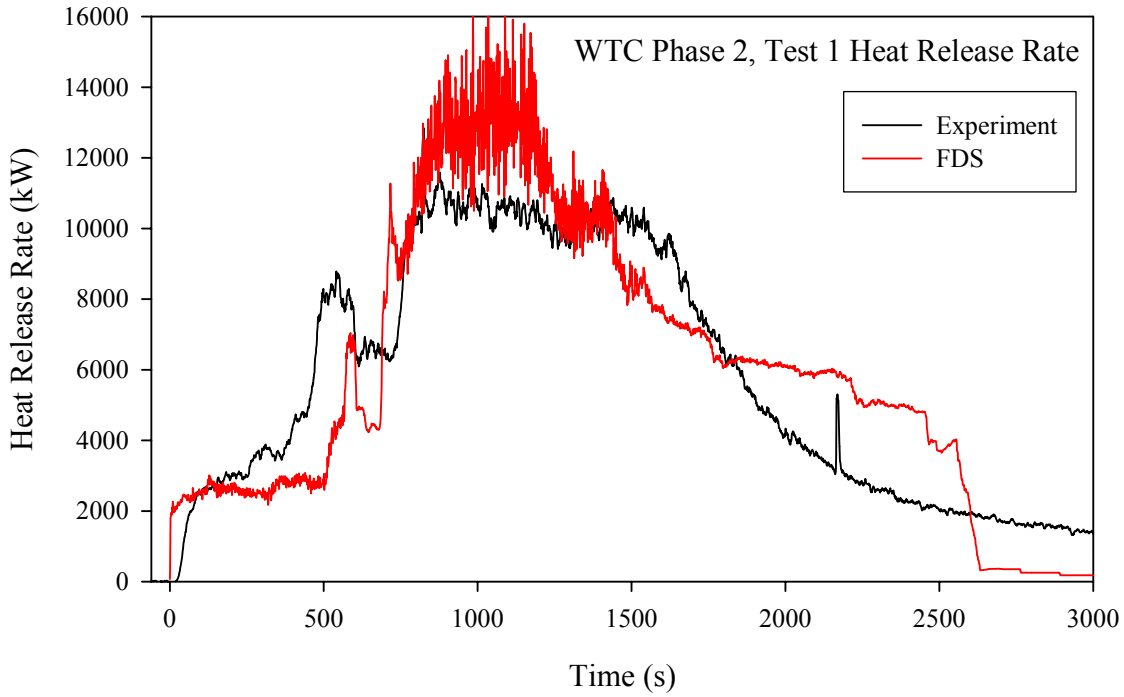

Figure 1–2. Comparison of HRR for Phase 2, Test 1.

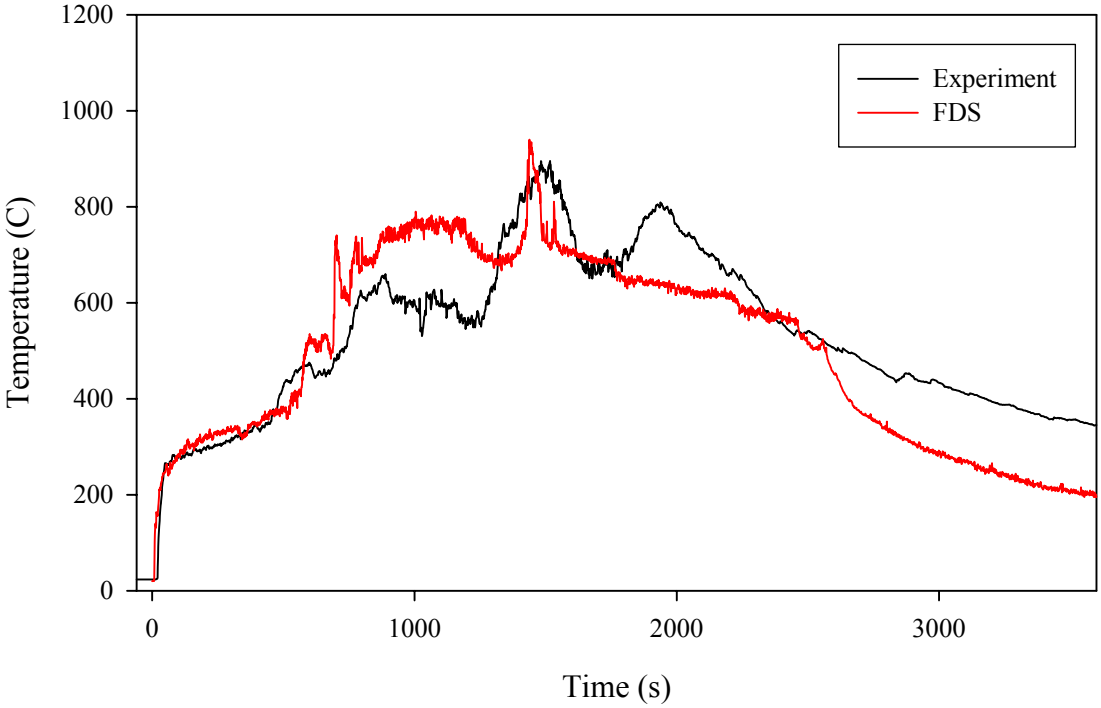

Figure 1–3. Upper layer gas temperature in the rear of the compartment, Phase 2, Test 1.

1.3 SIMULATIONS OF THE FIRES IN WTC 1 AND WTC 2

This section describes how the physical geometry of the buildings was described in the numerical model. Information about the layout of the relevant floors was obtained from architectural drawings provided by the occupants. For floors where information was not available, the geometry of a nearby floor or a floor of similar use was substituted. Information about exterior damage and window breakage was obtained by studying thousands of photographs and videos. There was no attempt made to predict the window breakage in the simulations. This information was provided as a boundary condition.

1.3.1 Numerical Grid

The windows in WTC 1 and WTC 2 were nominally spaced 1 m apart. In addition, the external columns plus their aluminum cladding were assumed to be 0.5 m wide. The slab-to-slab floor spacing was assumed to be 3.6 m. Because of these approximations, a uniform numerical mesh consisting of cells whose dimensions were 0.5 m × 0.5 m × 0.4 m was used. In the model, each tower face consisted of 58 windows, 61 columns, and two 0.5 m spacers next to each corner column. In the real tower geometry, these spacers formed the bevel. Figure 1–4 shows a single floor of the WTC 1 as it is approximated by the numerical model.

The numerical grid for each floor of WTC 1 and WTC 2 was of dimension 128 × 128 × 9 cells. The 128 cells in the horizontal directions allow for several meters of simulation outside of the external walls. The calculations were run in parallel, thus each floor was assigned to a different processor. The floor slabs, core walls, and workstations were approximated as thin obstructions. As described in the previous section, the contents of each workstation were collected into boxes and distributed throughout.

Penetrations in the floor slabs representing elevator shafts and HVAC ducts were created in the model by defining rectangular plates on top of the floor slab that were removed at the start of the calculation. This served to carve out holes in the floor. Window breakage was modeled by removing thin obstructions serving as windows at times obtained from the analysis of photographs and videos. Broken external columns were removed the same way.

1.3.2 Parallel Processing

Modeling the fires on multiple floors of WTC 1 and WTC 2 is computationally intensive, both in terms of CPU time and memory. Up to this point in its development, FDS has been limited to calculations small enough to run on a single CPU and fit into the memory of a desktop personal computer. The WTC study is an example of a large-scale fire modeling problem that is impossible to analyze without the use of parallel processing. In terms of parallelization, the exact details of FDS are not important. The approach taken to run the code on a cluster of machines can be applied to virtually any CFD code, in particular those that involve three spatial dimensions and time. In such cases, the computational demand is fairly well represented by the product of the number of computational grid cells and the number of time steps taken to advance the solution of the governing equations in time. For example, if the computational grid consists of 1 million cells and the simulation requires ten thousand time steps, the demand is 10^{10} cell-cycles. The overall demand can be broken down into memory requirement and CPU time. The memory requirement is a function of the number of grid cells; the CPU time is a function of the number of time steps.

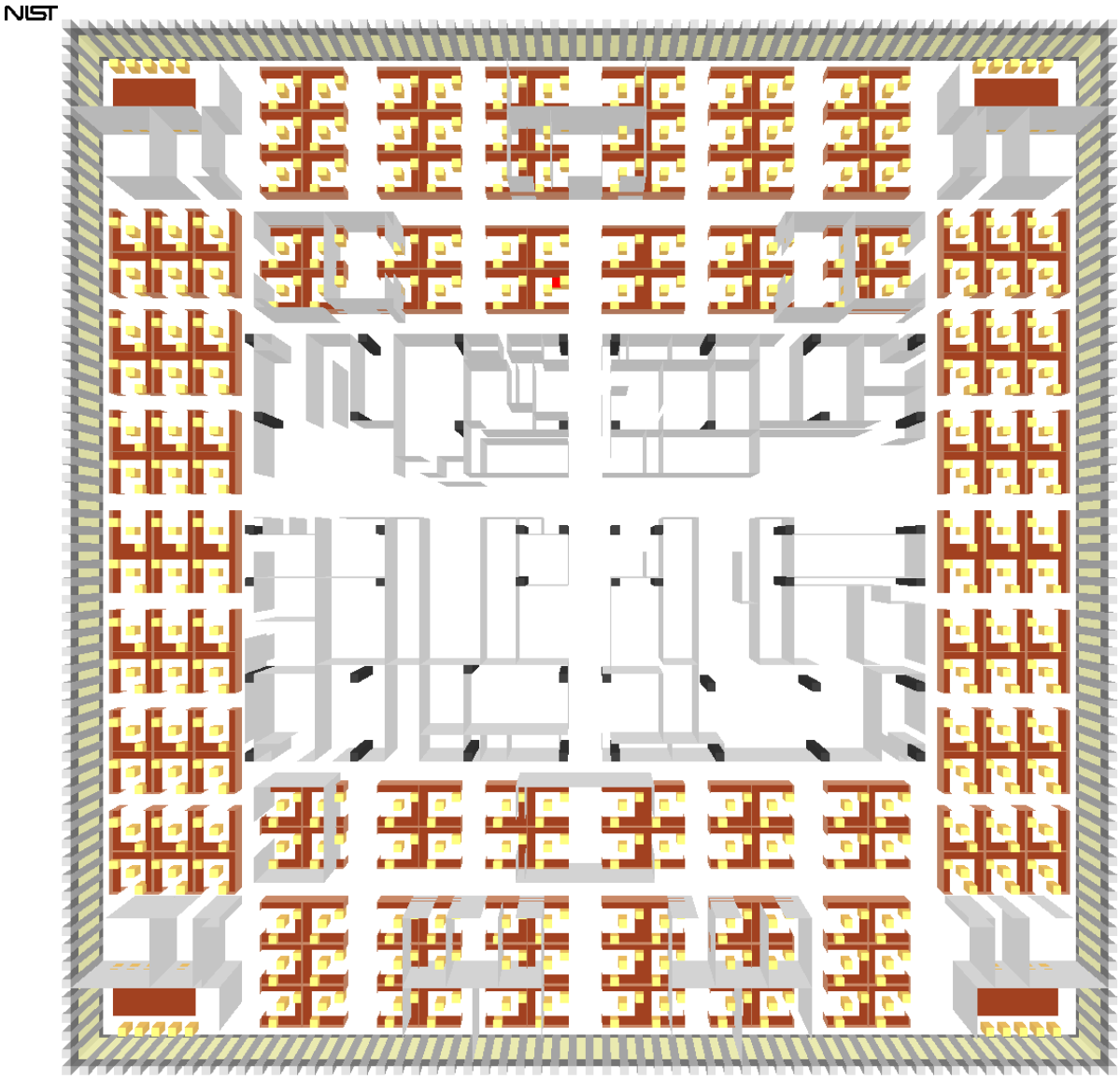

Figure 1–4. Plan view of a typical floor in WTC 1.

Roughly speaking, state of the art 32 bit processors can complete roughly 100,000 FDS cell-cycles per second. Realistic simulations of fires such as those in the WTC require on the order of 500,000,000,000 cell-cycles, or about two months of calculation on a single 2 GHz processor. Plus, the calculation would require 6 to 12 gigabytes of memory (RAM), well over the 4 gigabyte address space of 32 bit processors. Because of this, the WTC calculations are not only impractical on single processor systems, they are impossible on any 32 bit processor. A 64 bit processor system may theoretically handle the static memory requirements of a large simulation time, but the run times for large calculations remain prohibitive.

Because of the computational and memory issues of large fire simulations, a parallel version of the fire model must meet the two fundamental requirements discussed above, as well as satisfy a number of practical implementation concerns. Both the computational and the memory requirements must be distributed across multiple processors. The simulation must be done so that each processor uses less than

4 gigabytes of memory, while enough processors must be used to reduce the simulation to a practical length of time, of the order of one week.

Because the computational load is distributed throughout much of the source code, NIST has chosen to break up the calculation into multiple spatial blocks, with each block essentially doing the same type of calculation. A feature common to most CFD codes is multi-block or multi-mesh structure in which more than one structured grid is used in the calculation. This feature is exploited by simply putting the data and computation for each block on a different processor. This has advantages and some limitations. The advantages are (1) a natural and scalable extension of the existing code, (2) the amount of data communication will be kept to a minimum, since only overlap information needs to be communicated, rather than the data for full blocks, (3) source code changes are localized in small communication routines, (4) development is fairly fast. The disadvantages to the multi-block approach are (1) equal distribution of work across processors (load balancing) depends on spatial symmetry in the simulation, such as the translationally symmetric geometry of the WTC floors, (2) the level of parallelism and the speed up of the calculation is limited to the number of spatial blocks that can be used in the calculation. These limitations are not severe in many cases, including the WTC.

Because NIST is interested in a scalable, portable code, Message Passing Interface (MPI) is used. This is a standard, well-documented system of implementing parallel processing, that can work with shared memory, distributed memory, or combinations of those architectures (Gropp, 1999). Our goal in using MPI was to produce a code that, except for the requirement of the MPI library, would be as portable and standardized as the sequential version. The parallel code runs on most computer platforms, including networked Windows-based PCs. NIST opted for a cluster of commodity personal computers running Linux, connected by a gigabit ethernet network. The individual processors are in the range of 2.0 to 2.8 GHz, and dual processor machines were chosen to save space and to allow the addition of OpenMP code as a future extension to the MPI-based code. For production work in the NIST laboratory, two clusters are used: a smaller, development cluster to develop and debug the code, and a larger cluster with 128 processors. Using both clusters provides the capability to run six to eight large parallel processing jobs simultaneously.

1.3.3 Sample Simulation

Shown in Fig. 1–5 is a sequence of snapshots showing the predicted upper layer temperatures on a floor of WTC 1 at time increments of 15 min. The first image is a cut-away showing the damage to the north face of the tower and the layout of the walls and furnishings. The subsequent images are color coded by temperature, with the red (or dark) patches representing temperatures in the vicinity of 1,000 °C. Initially, these hot areas of active burning are near the impact zone at the north end (foreground of picture), but migrate towards the south as the combustible furnishings are exhausted. Driving the progress of the fires is the breaking of windows that provide air to the oxygen starved fire. The window breakage is not predicted by the model; it is an imposed boundary condition resulting from the analysis of thousands of photographs and videos recorded that day by eye witnesses. The uncertainty in the window break times is on the order of 5 min in areas not obscured by smoke.

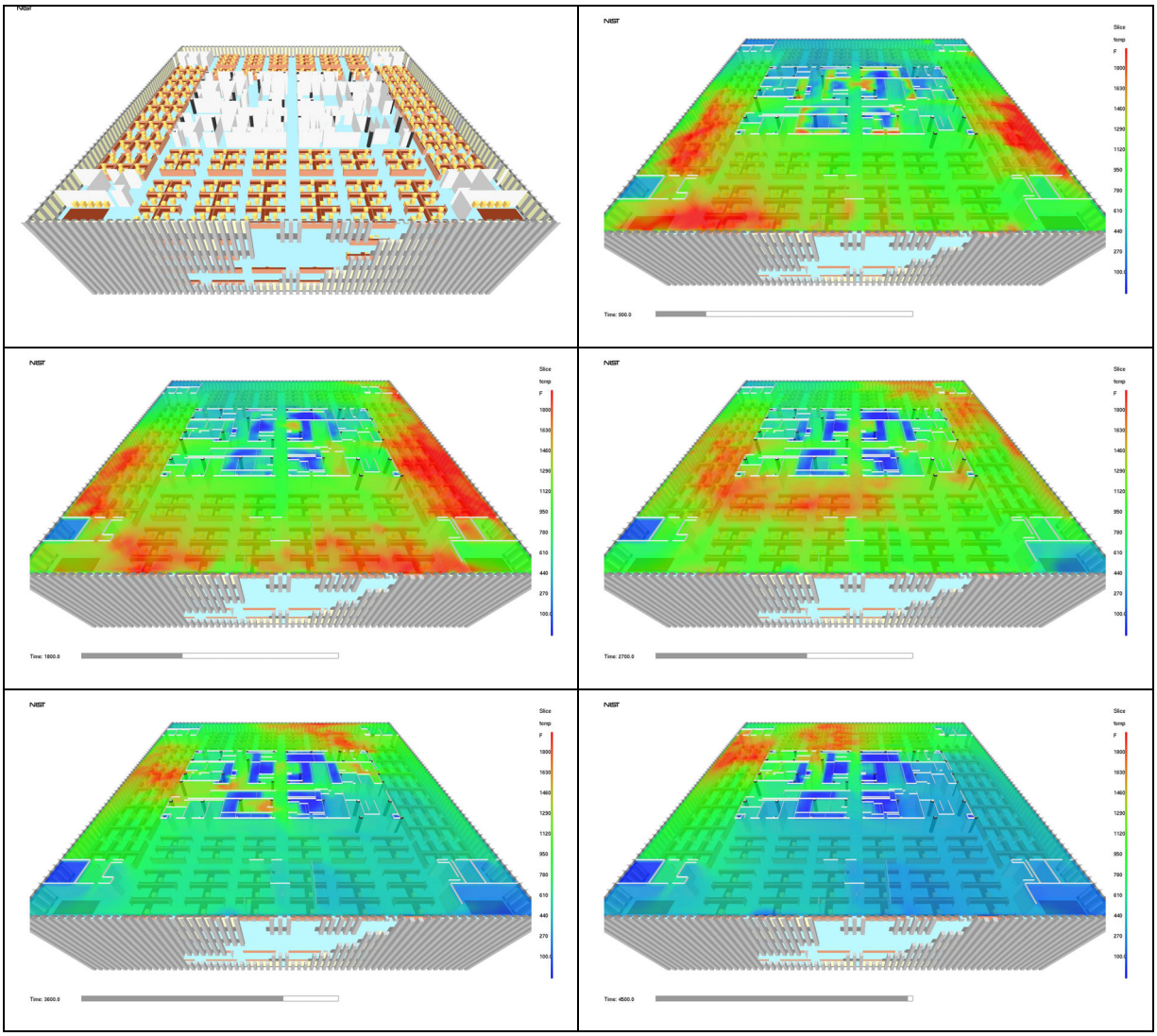

Figure 1–5. Predicted upper layer temperatures of a floor of WTC 1.

The burning behavior shown by the simulation is similar to that of the fires in experiments conducted by Ian Thomas and Ian Bennetts (1999). They looked at fire spread in long and wide enclosures with a single ventilation opening, where the fires were ignited at various points deep within the bench-scale compartments used. The fires would rapidly spread across the liquid or solid fuels covering the floor without consuming much of the fuel. The fires would then surround the compartment opening and burn back into the compartment as the fuel near the opening was exhausted. In the WTC simulations, fires are ignited over a wide area by simulated spray nozzles ejecting a liquid with properties of aircraft fuel. Much of the available oxygen is consumed rapidly, driving the fires to the openings created by the aircraft. The fires move away from the initial impact area as the nearby furnishings are exhausted, and as windows are broken out away in other parts of the building.

1.4 SUMMARY

The investigation into the cause of the collapse of WTC 1, WTC 2, and WTC 7 by NIST will not be completed until the fall of 2004. Work is on-going to simulate the weakening of the structural steel due to the aircraft impacts and the fires. Nevertheless, the fire experiments and simulations performed to date have improved our ability to analyze the response of any large building or structure to fire. In the years ahead, these techniques will become increasingly widespread due to faster computers and the ability to harness an entire set of off-the-shelf personal computers to perform very large calculations. Effective modeling is a combination of fast computers, efficient algorithms, and well-planned small and large scale experiments to provide both input to the model and a validation of results. Projects as complicated as the WTC study are rarely conducted using modeling alone. There is and will always be a need to coordinate computation and experiment to reconstruct the dynamics of large fires.

1.5 REFERENCES

Gropp, W., E. Lusk, and A. Skjellum. 1999. *Using MPI*, MIT Press, Cambridge, Massachusetts, USA.

Hamins, A., and K.B. McGrattan. 2003. Reduced-Scale Experiments on the Water Suppression of a Rack-Storage Commodity Fire for Calibration of a CFD Fire Model. Fire Safety Science: Proceedings of the Seventh International Symposium. International Association for Fire Safety Science.

McGrattan, K.B., H.R. Baum, R.G. Rehm, G.P. Forney, J.E. Floyd, K. Prasad and S. Hostikka. 2002. Fire Dynamics Simulator (Version 3), Technical Reference Guide. NISTIR 6783. National Institute of Standards and Technology, Gaithersburg, MD.

Ritchie, S.J., K.D. Steckler, A. Hamins, T.G. Cleary, J.C. Yang, and T. Kashiwagi. 1997. The Effect of Sample Size on the Heat Release Rate of Charring Materials. Fire Safety Science: Proceedings of the Fifth International Symposium. International Association for Fire Safety Science.

Thomas, I.R. and I.D. Bennetts. 1999. Fires in Enclosures with Single Ventilation Openings–Comparison of Long and Wide Enclosures. Fire Safety Science: Proceedings of the Sixth International Symposium. International Association for Fire Safety Science.

This page intentionally left blank.